

lncKRT16P6 promotes tongue squamous cell carcinoma progression by sponging miR-3180 and regulating GATAD2A expression

MI ZHANG^{1,2}, LING WU^{1,2}, XUDONG WANG^{1,2} and JIANG CHEN^{1,2}

¹School and Hospital of Stomatology and ²Fujian Key Laboratory of Oral Diseases of Fujian College and University, School and Hospital of Stomatology, Fujian Medical University, Fuzhou, Fujian 350002, P.R. China

Received April 1, 2022; Accepted July 5, 2022

DOI: 10.3892/ijo.2022.5401

Abstract. Tongue squamous cell carcinoma (TSCC) is characterized by a poor prognosis and its 5-year overall survival rate has not improved significantly. However, the precise molecular mechanisms underlying TSCC remain largely unknown. Through RNA screening, the present study identified a novel long noncoding RNA (lncRNA), keratin 16 pseudogene 6 (lncKRT16P6), which was upregulated in TSCC tissues and cell lines and associated with TSCC tumor stage and differentiation grade. Inhibition of lncKRT16P6 expression reduced TSCC cell migration, invasion and proliferation. lncKRT16P6 sponged microRNA (miR)-3180 and upregulated GATA zinc finger domain containing 2A (GATAD2A) expression. miR-3180 inhibition reversed the lncKRT16P6 depletion-induced attenuation of TSCC malignancy and GATAD2A depletion reversed the miR-3180 silencing-induced enhancement of TSCC malignancy. In summary, the present study revealed a potential competitive endogenous RNA (ceRNA) regulatory pathway in which lncKRT16P6 modulates GATAD2A expression by binding miR-3180, ultimately promoting tumorigenesis and metastasis in TSCC. Therefore, lncKRT16P6 may be used as a prognostic biomarker and therapeutic target for clinical intervention in TSCC.

Introduction

Tongue squamous cell carcinoma (TSCC) is one of the most common and lethal types of oral cancer (1) and is characterized by a poor prognosis, frequent lymphatic metastasis and a high rate of regional recurrence. Currently, the preferred

treatment for TSCC is surgery combined with postoperative radiotherapy and chemotherapy. However, the 5-year overall survival rate of TSCC has not improved significantly over the past decades (2). Diagnosing TSCC in the early stage is critical. Therefore, elucidating the molecular mechanisms underlying TSCC and exploring effective molecular therapeutic targets are essential for improving the survival rate of patients with TSCC.

Studies have confirmed numerous protein-coding genes and epigenetic factors that may regulate the microenvironment of cancer cells and tumors, such as long noncoding RNAs (lncRNAs), microRNAs (miRNAs/miRs) and histone modifications (3,4). Less than 2% of the human genome contains protein-coding genes and most transcripts are nonprotein-coding RNAs (5). Among these RNA transcripts are lncRNAs, which consist of >200 nucleotides and have been found to widely interact with biomacromolecules, such as DNA, RNA and proteins, to regulate fundamental cellular processes at the transcriptional or translational level (6). lncRNAs have diverse regulatory mechanisms in various cancers according to their subcellular localization. lncRNAs in the cytoplasm can function as competitive endogenous RNAs (ceRNAs). Since the structure of most lncRNAs is similar to that of mRNAs, miRNAs may negatively regulate the expression of lncRNAs through a mechanism similar to that of mRNAs. miRNAs play an important role in the posttranscriptional regulation of gene expression by degrading target gene mRNA or inhibiting the translation of mRNA and are widely involved in cell proliferation, differentiation and apoptosis and cell cycle regulation (7,8). In other words, lncRNAs can alleviate the repressive effect of miRNAs on mRNA expression by adsorbing miRNAs as sponges (9). In addition, lncRNAs can also interact with RNA-binding proteins (10). lncRNAs in the nucleus may be involved in the transcriptional regulation of genes (11).

The expression patterns of cancer-specific lncRNAs seem to be more tissue- and stage-specific than those of mRNAs, indicating that lncRNAs are promising alternative biomarkers and therapeutic targets (12). Dysregulated expression of lncRNAs has been reported in diverse pathologies, including TSCC and bladder, prostate, lung, breast and gastric cancers (13,14). For example, studies have shown that melatonin protects against

Correspondence to: Professor Jiang Chen, Fujian Key Laboratory of Oral Diseases of Fujian College and University, School and Hospital of Stomatology, Fujian Medical University, 88 Jiaotong Road, Fuzhou, Fujian 350002, P.R. China
E-mail: jiangchen@fjmu.edu.cn

Key words: long noncoding RNA, tongue squamous cell carcinoma, cell cycle, microRNA 3180, GATA zinc finger domain containing 2A

oral cancer cell migration through the epigenetic regulation of prune homolog 2 with BCH domain by inhibiting the expression and function of the lncRNA MROS-1 (15). The lncRNA colorectal neoplasia differentially expressed (CRNDE) is associated with the chemosensitivity of gastric cancer in an analysis of clinical samples and CRNDE directly binds the splicing protein SRSF6 to reduce its stability and thus regulate alternative splicing events (16). In addition, intricate interactions occur between coding and noncoding RNAs. These two types of RNA transcripts can serve as ceRNAs, *i.e.*, miRNA sponges, to precisely regulate signaling networks by competing for shared miRNAs and thus significantly effect tumorigenesis and development (17). For example, the lncRNA ESCCAL-1 promotes the invasion and migration of esophageal squamous cell carcinoma cells by reducing the inhibitory effect of miR-590-3p on APOBEC3G expression (18). A study has identified that FAM225A, an oncogenic lncRNA, enhances ITGB3 expression and activation of the focal adhesion kinase/PI3K/Akt pathway by sponging miR-590-3p and miR-1275, thereby promoting the malignant features of nasopharyngeal carcinoma (19). The lncRNA Cardiac Mesoderm Enhancer-associated Noncoding is a predictive biomarker and the host gene of miR143-3p, which downregulates MCM5, inhibiting DNA replication in breast cancer (20). Studies have also identified several lncRNAs that can modulate various aspects of diverse biological processes in TSCC, including cell proliferation, tumorigenesis, cell survival, apoptosis and cell migration (21-23). However, although thousands of lncRNAs have been identified, the biological functions and underlying regulatory mechanisms of lncRNAs in tongue cancer progression remain largely elusive. Thus, further insight into lncRNA-dependent gene-regulatory mechanisms will provide predictive biomarkers and individual treatments for TSCC.

The present study, based on our previous research results (24), performed an in-depth analysis of lncRNA expression profiles and identified a novel lncRNA, keratin 16 pseudogene 6 (lncKRT16P6), which was upregulated in TSCC tissues and cell lines and associated with TSCC tumor stage and differentiation grade. The aim of the present study was to explore the specific regulatory mechanism by which lncKRT16P6 promoted the occurrence and development of TSCC. To this end, after *in vitro* and *in vivo* functional experiments such as CCK-8, Transwell, clone formation, flow cytometry, fluorescence *in situ* hybridization (FISH), dual luciferase report experiments, it was found that lncKRT16P6 promoted TSCC cell proliferation and metastasis. In addition, as a ceRNA, lncKRT16P6 sponged miR-3180 to increase GATA zinc finger domain containing 2A (GATAD2A) expression. The present study elucidated the clinical significance and regulatory mechanism of lncKRT16P6 in TSCC and provides a prognostic indicator for TSCC patients as well as a promising therapeutic target for TSCC.

Materials and methods

Clinical samples and ethical approval. A total of 50 pairs of tongue cancer specimens were collected from patients who underwent surgery at the First Affiliated Hospital of Fujian Medical University (Fuzhou, Fujian, China) between January 2017 and January 2020. The School and Hospital of

Stomatology and the First Affiliated Hospital are cooperative units affiliated with Fujian Medical University. All samples were immediately snap frozen in liquid nitrogen and stored at -80°C until needed. Two pathologists pathologically confirmed each sample by hematoxylin-eosin (HE) staining. Written informed consent was obtained from all participants in accordance with the Declaration of Helsinki and the study protocol was approved by the Ethics Committee of the First Affiliated Hospital of Fujian Medical University [approval number: No. 159 (2020) of the First Affiliated Hospital of Fujian Medical University] The clinicopathological characteristics of the patients are summarized in Table I.

Cell lines and cell culture. TSCC cell lines CAL-27 and SCC-9 were purchased from the American Type Culture Collection and normal human oral keratinocyte (HOK) cells were generously donated by the research group of Professor Cheng Hui, School of Stomatology, Fujian Medical University. The primary HOK cells were purchased from ScienCell Research Laboratories Inc. In order to acquire adequate cells for the subsequent study, the immortalization of HOK was conducted. HOK were maintained in oral keratinocyte medium (OKM; ScienCell Research Laboratories Inc.) before proceeding with immortalization. The primary HOK were infected by hTERT retrovirus expressing simian virus 40 large T antigen (SV40-T). Once the infection of HOK was performed, the immortalized cells were subsequently selected and passaged with OKM changed every 3 days (25). CAL-27 cells and HOK cells were grown in DMEM (Gibco; Thermo Fisher Scientific, Inc.) supplemented with 10% FBS (Gibco; Thermo Fisher Scientific, Inc.). SCC-9 cells were cultured in DMEM/F-12 (Gibco; Thermo Fisher Scientific, Inc.) supplemented with 10% FBS and $0.4\ \mu\text{g}/\text{ml}$ hydrocortisone. The pH of the cell culture medium was 7.0 to 7.4. All cells were maintained at 37°C in an incubator supplied with 5% CO_2 .

RNA preparation and reverse transcription-quantitative (RT-q) PCR. Total RNA was extracted from tissues or cells using TRIzol[®] reagent (Thermo Fisher Scientific, Inc.) according to the manufacturer's instructions. The cell density for RNA extraction was 1×10^6 . The concentration and purity of RNA were evaluated using a Quawell spectrophotometer (Q5000; Quawell Technology, Inc.). When the 260/280 ratio of RNA was >1.8 , total RNA was reverse transcribed into cDNA using a PrimeScript RT reagent kit (Takara Biotechnology Co., Ltd.) according to the manufacturer's instructions. RT-qPCR analyses were performed using SYBR Green Master Mix (Takara Biotechnology Co., Ltd.) in an Applied Biosystems 7500 Real-Time PCR System (Applied Biosystems; Thermo Fisher Scientific, Inc.) according to the manufacturer's instructions. PCR cycling conditions were: Pre-denaturation: 95°C , 1 min; denaturation: 95°C , 15 sec; annealing: 60°C , 30 sec; extension: 72°C , 1 min; 72°C , 10 min for a total of 40 cycles. Target mRNA expression levels were normalized to that of glyceraldehyde-3-phosphate dehydrogenase (GAPDH). Relative expression levels were calculated by the $2^{-\Delta\Delta\text{C}_q}$ method (26). All experiments were repeated three times. MiR-mimics NC, hsa-miR-3180 mimics, miR-inhibitor NC and hsa-miR-3180 inhibitor were designed and synthesized by Shanghai GenePharma Co., Ltd. and the primers were

Table I. Correlations between the expression level of lncKRT16P6 and the clinicopathological characteristics of TSCC patients.

Characteristics	Cases	High expression level (n=25)	Low expression level (n=25)	P-value (χ^2)
Age (years)				0.155969 (2.012882)
≥60	23	14	9	
>60	27	11	16	
Sex				0.122823 (2.380952)
Male	35	15	20	
Female	15	10	5	
Tumor stage				0.020921 ^a (5.333333)
I-II	20	14	6	
III-IV	30	11	19	
T stage				0.575027 (1.987395)
T1	4	4	0	
T2	17	14	3	
T3	8	6	2	
T4	21	18	3	
N stage				0.275065 (3.876923)
N0	30	25	5	
N1	6	5	1	
N2	13	11	2	
N3	1	1	0	
Differentiation grade				0.041399 ^a (4.159593)
High	19	13	6	
Moderate-poor	31	12	19	

^aP<0.05. lnc, long noncoding RNA; TSCC, tongue squamous cell carcinoma.

provided by Fuzhou Sunya Biotechnology, Co., Ltd. and are listed in Table SI.

Small interfering RNAs (siRNAs) and lentiviral transduction. siRNAs targeting lncKRT16P6 and GATAD2A were designed and synthesized by Shanghai GenePharma Co., Ltd. (sequences listed in Table SII). The two siRNAs with the best knockdown efficiency were used in subsequent functional studies. The cell density of CAL-27 and SCC-9 cells for transfection was 2×10^5 . The mass of mimic, vector and si-NC used for transfection were 50 pmol. The transfection reagent was Lipofectamine[®] 3000 (Thermo Fisher Scientific, Inc.) and the dosage for each well of a 6-well plate was 5 μ l. Cell transfection steps were performed according to the product manual. Diluted Lipofectamine[®] 3000 (Thermo Fisher Scientific, Inc.) in Opti-MEM Medium (Gibco; Thermo Fisher Scientific, Inc.) and mixed well. The master mix of DNA was prepared by diluting DNA in Opti-MEM Medium and mixing well. Diluted DNA was added to each tube of diluted Lipofectamine[®] 3000 (Thermo Fisher Scientific, Inc.; 1:1 ratio). After incubation for 20 min at room temperature DNA-lipid complex was added to the cells. Cells were incubated for 48 h at 37°C before subsequent experiments. For lentiviral transduction, virus-containing supernatant was collected 48 h after cotransfection of the packaging plasmids pGag/Pol and pRev, the envelope plasmid pVSV-G (Shanghai GenePharma Co., Ltd.)

and the short hairpin RNA (shRNA; shlncKRT16P6) vector or empty vector as control into 293(T) cells and the lentiviral vectors were then transduced into the target cells. The lentiviral vector pLV3/H1/GFP&Puro was constructed by Shanghai GenePharma Co., Ltd. To establish stable cell lines, tongue cancer cells were transduced with the above lentiviral vectors in the presence of polybrene (5 μ g/ml, Shanghai GenePharma Co., Ltd.). After incubation for 72 h, cells were selected with 2 μ g/ml puromycin (GeneChem) for 3 days. Information on the viral vectors and verification of the transduction efficiency are shown in Fig. S1.

Cell counting kit-8 (CCK-8) assay. The different groups of treated CAL-27 and SCC-9 cells (1,000) were seeded into each well of a 96-well plate. Cell viability was determined every 24 h using a CCK-8 assay (Dojindo Laboratories, Inc.) by measuring the absorbance of the different cell cultures at 450 nm (BioTek Instruments, Inc.), in accordance with the manufacturer's instructions. The proliferation of CAL-27 and SCC-9 cells expressing control or lncKRT16P6 siRNA was detected by CCK-8 assays, CCK-8 assays were performed in CAL-27 and SCC-9 cells stably transfected with sh-lncKRT16P6 with or without the miR-3180 inhibitor and CCK-8 assays were performed in CAL-27 and SCC-9 cells transfected with the miR-3180 inhibitor with or without GATAD2A siRNAs.

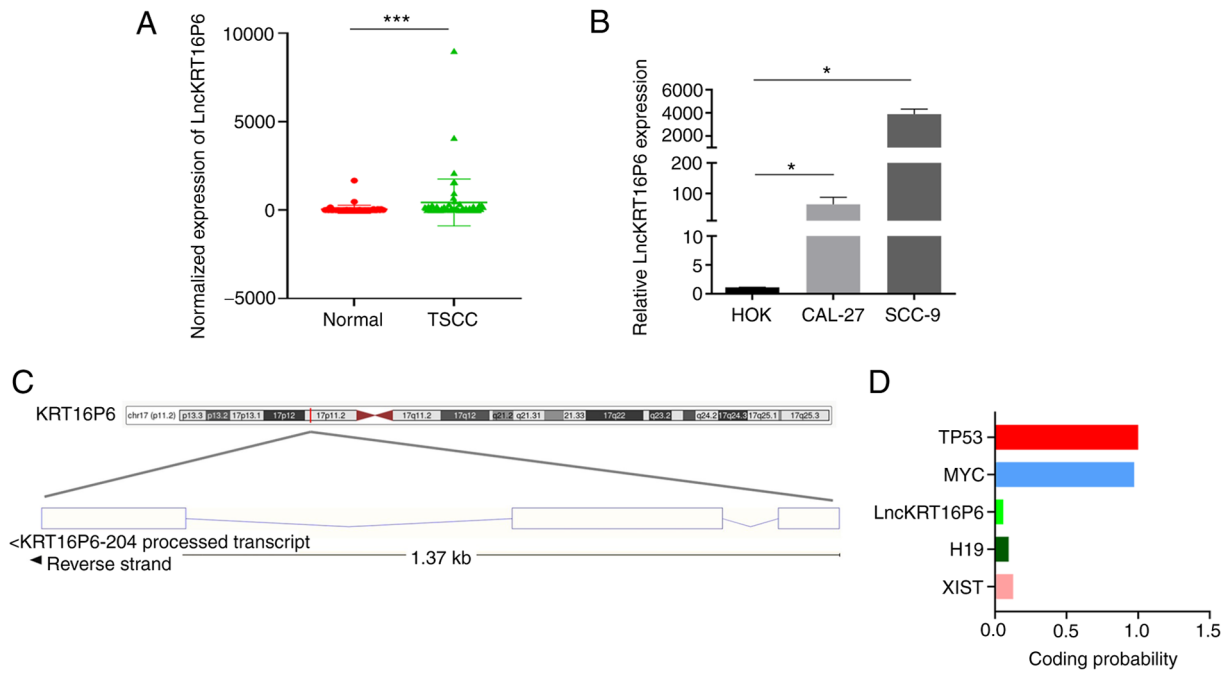


Figure 1. lncKRT16P6 expression is upregulated in TSCC tissues and is associated with TSCC progression. (A) Normalized expression of lncKRT16P6 in 50 pairs of TSCC tissues and adjacent normal tissues determined by RT-qPCR analysis. (B) RT-qPCR analysis of lncKRT16P6 expression in tongue cancer cell lines and HOK cells. (C) Location of lncKRT16P6, as determined with the Ensembl database. (D) Relative coding probability of lncKRT16P6, as determined by Coding Potential Calculator 2. All data are presented as the mean \pm standard error of the mean of three independent experiments. * $P < 0.05$, *** $P < 0.001$. lnc, long noncoding RNA; TSCC, tongue squamous cell carcinoma; RT-qPCR, reverse transcription-quantitative PCR.

Transwell assays. The invasive and migratory capacities of cells were evaluated using Transwell chambers with 8- μ m pore filters. After 48 h of transfection, cells in serum-free medium (5×10^4 cells/100 μ l) were plated in the upper chambers, which contained membranes coated with or without 50 μ l of Matrigel (BD Biosciences) at 37°C for 2 h. DMEM containing 10% FBS was added to the lower chambers as a chemoattractant. After incubation for 12 h at 37°C, cells that had migrated to the bottom surface of the membrane were fixed with 4% paraformaldehyde at room temperature for 30 min and stained with a crystal violet solution at room temperature for 10 min. Cells in five random fields were counted and the numbers were averaged.

Colony formation assays. Transfected cells (1×10^3) were uniformly seeded in 6-well plates and cultured for 2 weeks at 37°C in an incubator supplied with 5% CO₂, then the colony formation of the cells was observed under a low magnification (x10) microscope. The number of cells >10 were counted as a colony, and then the number of colonies in different treatments counted. The cells were then washed with phosphate-buffered saline (PBS), fixed with 4% paraformaldehyde at room temperature for 30 min, stained with 0.5% crystal violet at room temperature for 10 min and images captured.

Flow cytometry. Cells were routinely transfected and cultured for 48 h and were then digested with EDTA-free trypsin. An Annexin V-fluorescein isothiocyanate (FITC) apoptosis assay kit (BD Biosciences) was used to estimate the apoptosis rate according to the manufacturer's instructions. Cells were suspended in 1X Annexin binding buffer and 5 μ l of Annexin V reagent and 3 μ l of propidium iodide (PI) reagent were then added to 100 μ l of the cell suspension and mixed.

The mixture was incubated in the dark for 30 min at room temperature and 400 μ l of 1X Annexin binding buffer was then added to each sample to terminate staining.

For cell cycle analysis, a PI/RNase staining kit (BD Biosciences) was used according to the manufacturer's instructions. After treatment, tongue cancer cells were harvested, washed with ice-cold PBS and fixed with 70% ethanol for 24 h at 4°C. After staining with PI in the dark for 30 min at 4°C, the apoptosis rate (the percentage of late apoptotic cells) and cell cycle distribution were evaluated using a FACSVerse flow cytometer (BD Biosciences).

RNA FISH. Cy3-labeled probes specific for lncKRT16P6 were designed and synthesized by Shanghai GenePharma Co., Ltd. Probe signals were detected with a FISH kit (Shanghai GenePharma Co., Ltd.) according to the manufacturer's instructions. In brief, cells were fixed, permeabilized (1X PBS/0.5% Triton X-100) and prehybridized. Then, the cells were hybridized in hybridization buffer with Cy3-labeled probes specific for lncKRT16P6 at 37°C overnight. Cells were sequentially rinsed with 4X SSC (containing 0.1% Tween 20), 2X SSC and 1X SSC at 42°C and nuclei were stained with 4',6-diamidino-2-phenylindole (DAPI) (Beyotime Institute of Biotechnology). Probe signals were observed via fluorescence microscopy, the (magnification, x630). The probe sequences are listed in Table SIII.

Cell nucleocytoplasmic fractionation. Cell nucleocytoplasmic fractionation was performed with a Nuclear and Cytoplasmic Protein Extraction kit and RNase Inhibitor (Beyotime Institute of Biotechnology,) according to the manufacturer's instructions. Cytoplasmic and nuclear RNA was separated from tongue

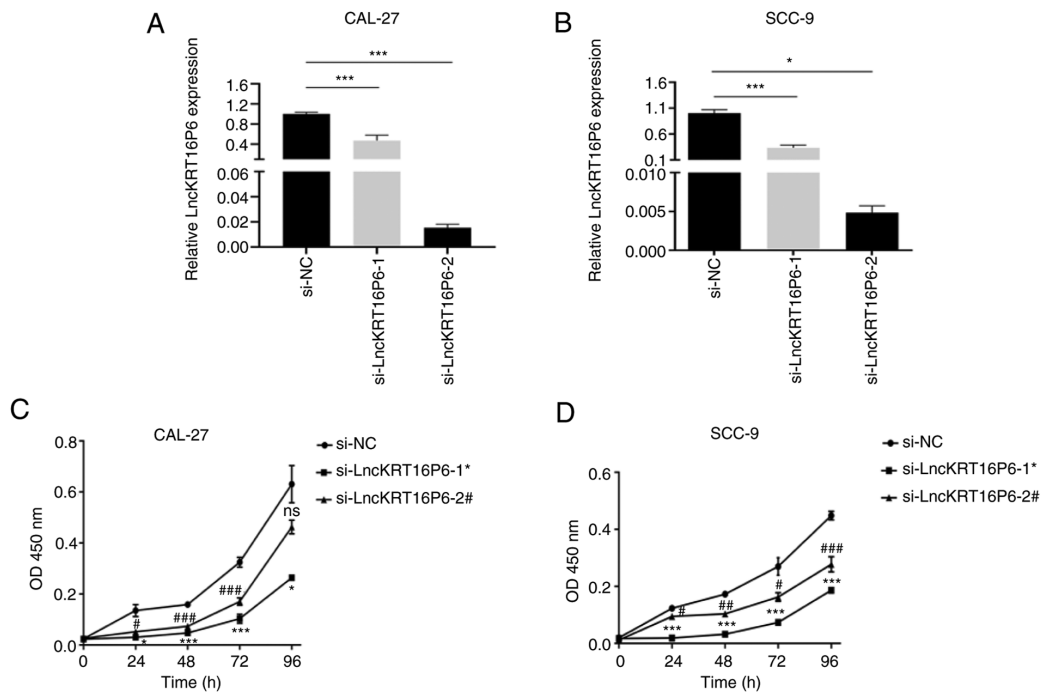


Figure 2. IncKRT16P6 promotes TSCC proliferation *in vitro*. (A) IncKRT16P6 expression in CAL-27 and (B) SCC-9 cells transfected with two specific IncKRT16P6 siRNAs was examined by reverse transcription-quantitative PCR. (C) The proliferation of CAL-27 and (D) SCC-9 cells expressing control or IncKRT16P6 siRNA was detected by CCK-8 assays. All data are presented as the mean \pm standard error of the mean of three independent experiments. * P <0.05, *** P <0.001. # P <0.05, ## P <0.01, ### P <0.001. Inc, long noncoding RNA; si, short interfering; TSCC, tongue squamous cell carcinoma; NC, negative control.

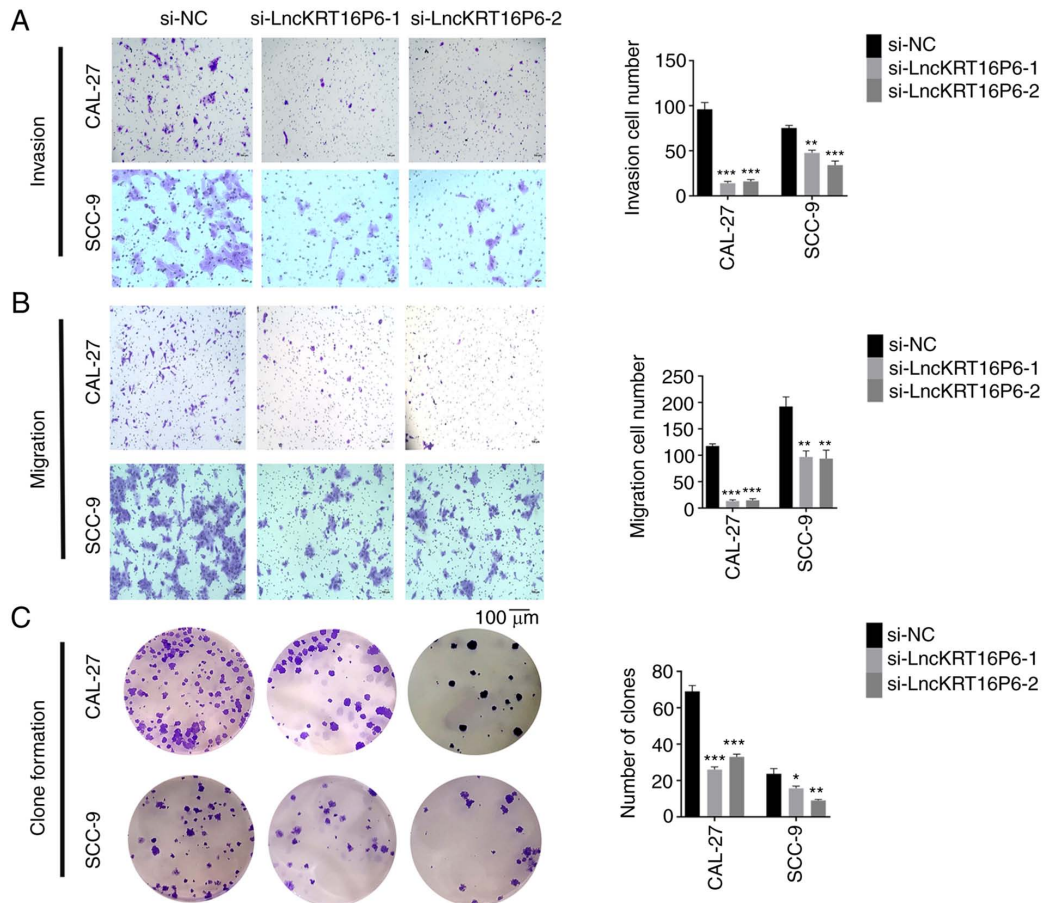


Figure 3. IncKRT16P6 promotes TSCC progression *in vitro*. (A) Representative images and quantitative analysis of the invasion, (B) migration and (C) colony formation of CAL-27 and SCC-9 cells expressing control or IncKRT16P6 siRNAs were detected by Transwell and colony formation assays. Scale bar=100 μ m. All data are presented as the mean \pm standard error of the mean of three independent experiments. * P <0.05, ** P <0.01, *** P <0.001. Inc, long noncoding RNA; TSCC, tongue squamous cell carcinoma; NC, negative control; si, short interfering.

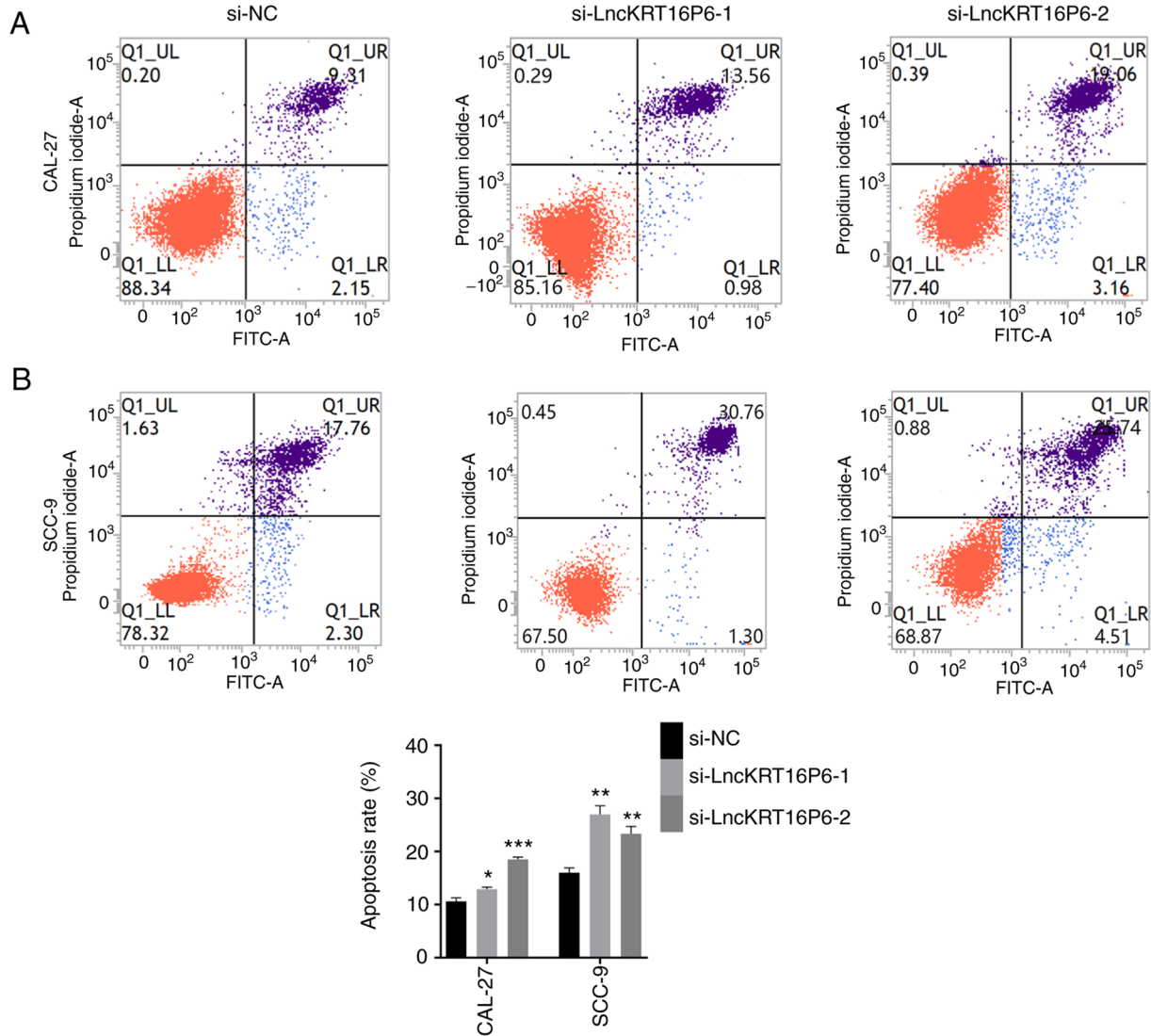


Figure 4. lncKRT16P6 inhibits the apoptosis of TSCC cells. (A) Representative images and quantitative analysis of apoptosis in CAL-27 and (B) SCC-9 cells expressing control or lncKRT16P6 siRNAs detected by flow cytometry. All data are presented as the mean \pm standard error of the mean of three independent experiments. * $P < 0.05$, ** $P < 0.01$, *** $P < 0.001$. lnc, long noncoding RNA; TSCC, tongue squamous cell carcinoma; NC, negative control; si, short interfering.

cancer cells and reverse transcribed. The lncKRT16P6 level was evaluated by RT-qPCR as aforementioned and its percentages in the nuclear and cytoplasmic fractions were determined.

Xenograft tumor formation and staining. The Animal Experimentation Ethics Committee of Fujian Medical University approved the present study and ensured that all experiments conformed to all relevant regulatory standards (approval number: FJMU IACUC NO. 2020-0039 of Fujian Medical University). In the present study, 4-week-old BALB/c athymic male nude mice (Shanghai SLAC Laboratory Animal Co., Ltd.) were used. The weight of nude mice was $\sim 20 \pm 5$ g. All mice were maintained under controlled temperature ($22 \pm 1^\circ\text{C}$) and humidity ($50 \pm 5\%$) in a 12 h light/dark cycle with food and water available ad libitum. CAL-27 cells (5×10^6 cells/ $100 \mu\text{l}$) transfected with different constructs were subcutaneously injected into the nude mice. A total of eight mice were randomly divided into two groups: i) sh-NC group (control group, mice were injected subcutaneously with CAL-27 cells transfected with empty vector, $n=4$); ii) sh-lncKRT16P6 group (mice were injected subcutaneously

with CAL-27 cells transfected with sh-lncKRT16P6, $n=4$). Tumors were measured weekly and the tumor volume (V) was calculated using the equation $V = (L \times W^2) / 2$, where L and W were the length and width of the tumor, respectively. After 24 days, the mice were sacrificed; 1% pentobarbital sodium 40 mg/kg was injected intraperitoneally and the animals were sacrificed by acute exsanguination after they became unconscious. The tumors were excised for hematoxylin and eosin (HE) and immunohistochemical (IHC) staining.

For HE staining, in brief, paraffin-embedded tumor tissues were sliced into $4\text{-}\mu\text{m}$ -thick sections. Deparaffinized and rehydrated sections were stained with HE (Beyotime Institute of Biotechnology) at room temperature for 5 min and the stained tissues were evaluated under a light microscope (magnification, $\times 100$ and $\times 200$). For IHC staining, the Ready-to-use Immunohistochemical UltraSensitive SP Detection kit (Mouse/Rabbit; Fuzhou Maixin Biotech Co., Ltd.) and Enhanced DAB Plus kit (Fuzhou Maixin Biotech Co., Ltd.) were used according to the manufacturer's instructions. Paraffin-embedded tumor sections ($4\text{-}\mu\text{m}$ -thick) were deparaffinized and blocked

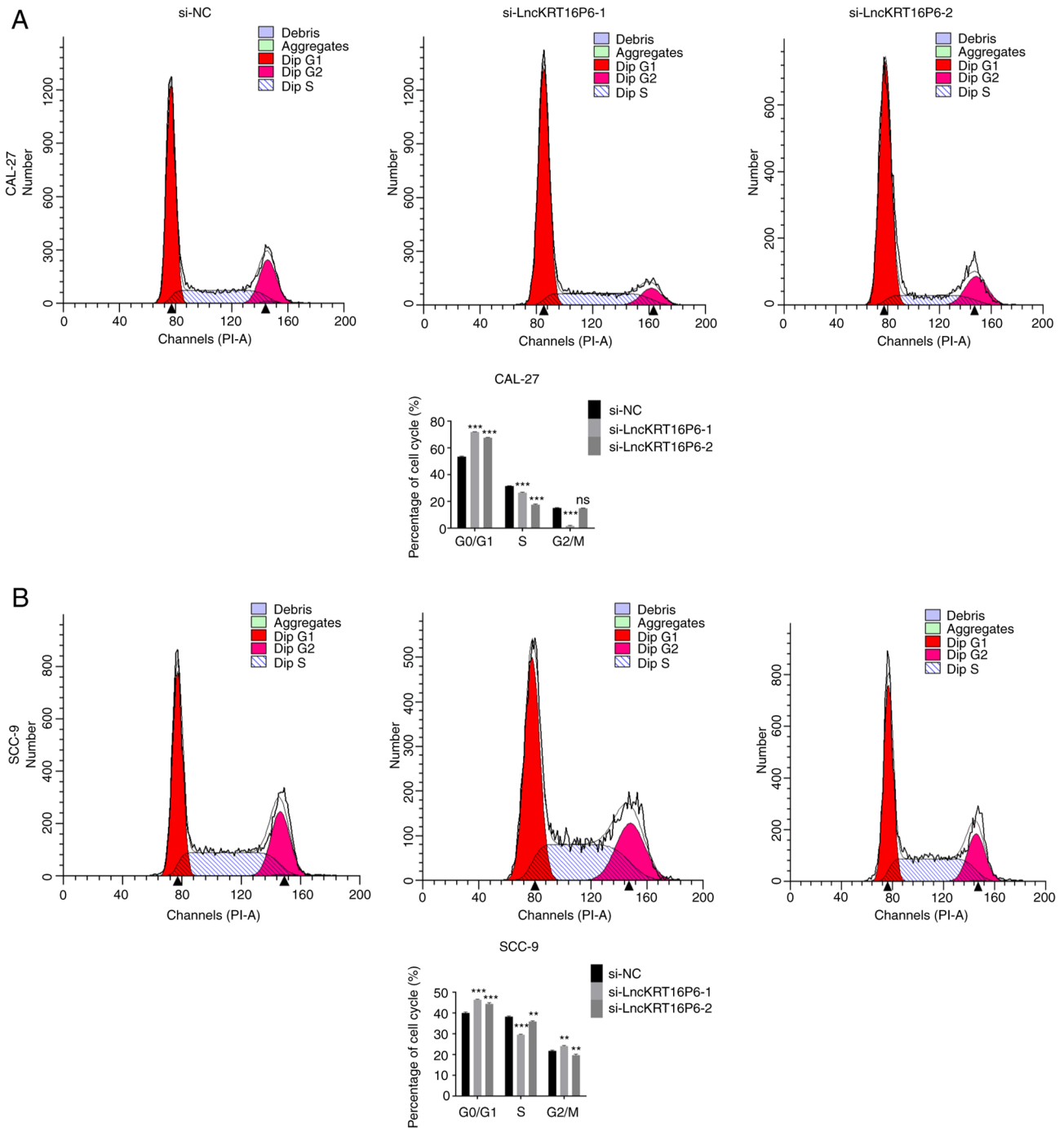


Figure 5. lncKRT16P6 regulates the cell cycle in TSCC cells. (A) Representative images and quantitative analysis of cell cycle progression in CAL-27 and (B) SCC-9 cells expressing control or lncKRT16P6 siRNAs detected by flow cytometry. All data are presented as the mean \pm standard error of the mean of three independent experiments. ** $P < 0.01$, *** $P < 0.001$. Inc, long noncoding RNA; TSCC, tongue squamous cell carcinoma; NC, negative control; si, short interfering.

with 5% goat non-immune serum (UltraSensitive SP kit; Fuzhou Maixin Biotech Co., Ltd.) and incubated at room temperature for 10 min. Primary antibodies were diluted in bovine serum albumin and the sections were then incubated with the anti-Ki67 antibody (1:500; Fuzhou Maixin Biotech Co., Ltd.) overnight at 4°C in a wet chamber. Then the tumor sections were incubated with secondary antibodies (UltraSensitive SP kit; Fuzhou Maixin Biotech Co., Ltd.) at room temperature for 10 min, diaminobenzidine reagent was added and hematoxylin counterstaining was performed to visualize nuclei.

Bioinformatic analysis. Interaction probabilities between lncRNAs and miRNAs were predicted using the online *in silico* tool MicroRNA Target Prediction Database (miRDB 6.0; <http://mirdb.org/>). Interaction probabilities between miRNAs and mRNAs were analyzed using online *in silico* tools, including miRDB, the Encyclopedia of RNA Interactomes (ENCORI 3.0, also known as StarBase; <https://starbase.sysu.edu.cn/index.php>), Prediction of MicroRNA Targets (TargetScan 3.1; http://www.targetscan.org/mamm_31/) and MicroRNA-Target Interactions (miRTarBase 9.0

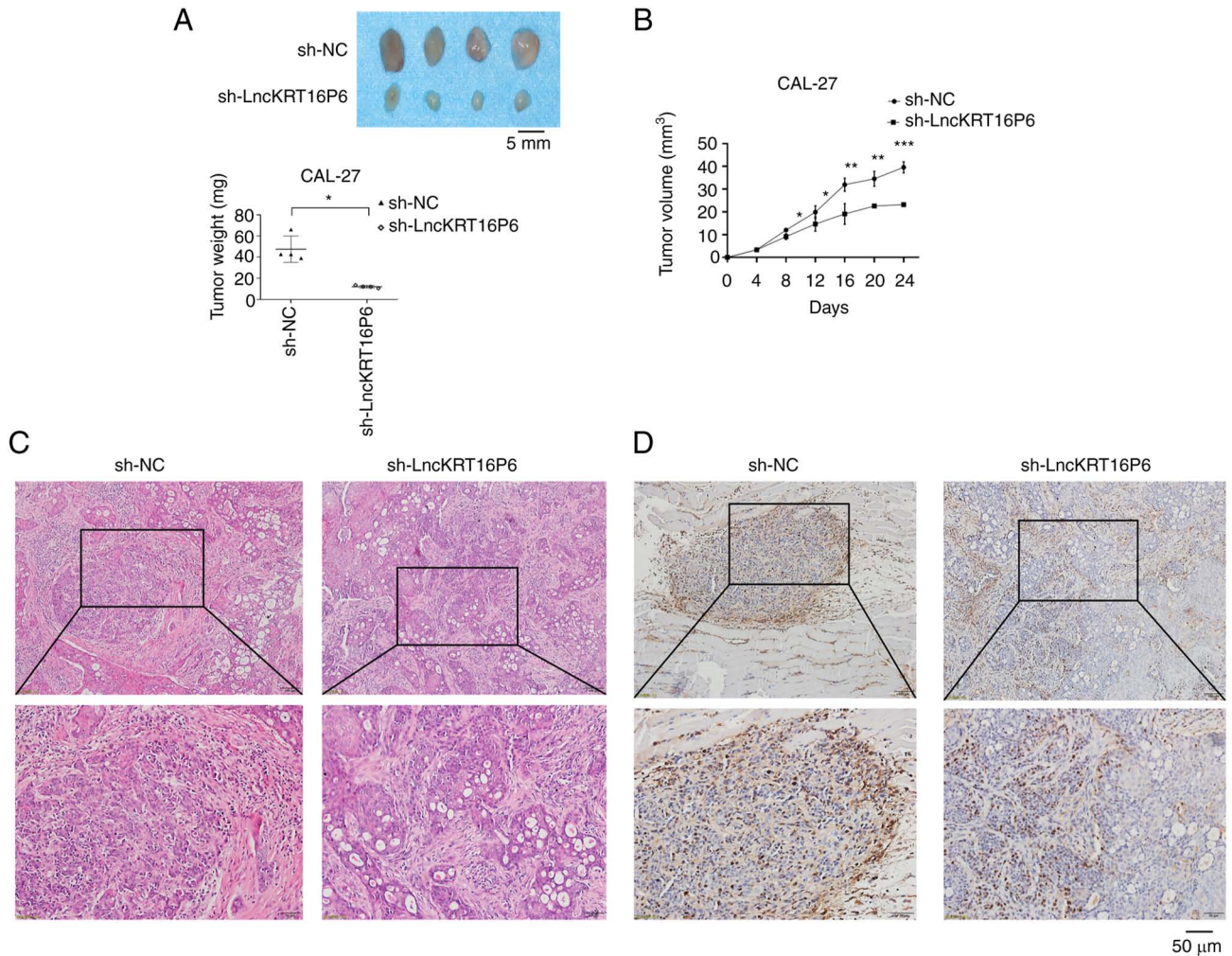


Figure 6. lncKRT16P6 promotes TSCC progression *in vivo*. (A) Representative images of subcutaneous tumors and tumor weights in a subcutaneous tumorigenesis experiment in nude mice. Scale bar=5 mm. (B) Analysis of subcutaneous tumor growth in different groups during a subcutaneous tumorigenesis experiment in nude mice (n=4 mice per group). Representative images of cell proliferation activity, as indicated by (C) hematoxylin and eosin and (D) immunohistochemical staining for Ki-67, in subcutaneous tumors in the lncKRT16P6 knockdown group and the corresponding control group. Scale bar=50 μ m. All data are presented as the mean \pm standard error of the mean of three independent experiments. *P<0.05, **P<0.01, ***P<0.001. lnc, long noncoding RNA; TSCC, tongue squamous cell carcinoma; NC, negative control; si, short interfering.

beta; https://mirtarbase.cuhk.edu.cn/~miRTarBase/miRTarBase_2022/php/index.php). Ensembl database (Ensembl 104; <http://asia.ensembl.org/index.html>) was used to identify the location of lncKRT16P6 and its sequence was predicted to exhibit lower protein-coding potential by Coding Potential Calculator 2 (CPC 2.0; <http://cpc2.gao-lab.org/>).

Dual-luciferase reporter assay. This experiment used the Dual-Luciferase reporter gene detection system kit (Promega Corporation), which was used according to the manufacturer's instructions. GP-transfect-Mate transfection reagent (Shanghai GenePharma Co., Ltd.) was used for transfection. Cells were seeded in 12-well plates at a density of 5×10^5 cells per well for 24 h before transfection. Reporter plasmids [pGP-miRGLO-Firefly luciferase-Renilla luciferase, containing lncKRT16P6, the GATAD2A 3' untranslated region (UTR), or the corresponding mutant (MUT) sequences] were designed by Shanghai GenePharma Co., Ltd. 293(T) cells were cotransfected with a reporter plasmid and either miR-3180 mimic or the NC mimic (Shanghai GenePharma Co., Ltd.).

After 48 h, luciferase activity was measured using a dual-luciferase reporter assay system (Promega Corporation) according to the manufacturer's protocol. Firefly luciferase activity was normalized to Renilla luciferase activity.

Western blot analysis. Cells were prepared at 4°C in radioimmunoprecipitation assay (RIPA) buffer containing phenylmethylsulfonyl fluoride (PMSF; Beijing Solarbio Science & Technology Co., Ltd.). Then, the protein concentration was determined using the BCA kit (Beyotime Institute of Biotechnology). Proteins (25 μ g per lane) were electrophoretically separated on 10% SDS-PAGE gels and transferred onto polyvinylidene difluoride membranes. The membrane was placed in 5% non-fat milk (Hangzhou Fude Biological Technology Co., Ltd.) and blocked for 3 h at room temperature to remove nonspecific binding sites. Membranes were then incubated with the appropriate primary antibodies overnight at 4°C, and incubated with the appropriate secondary antibodies at room temperature for 30 min. Primary antibodies specific for the following proteins were used: E-cadherin (1:1,000; cat. no. 3195; CST Biological Reagents

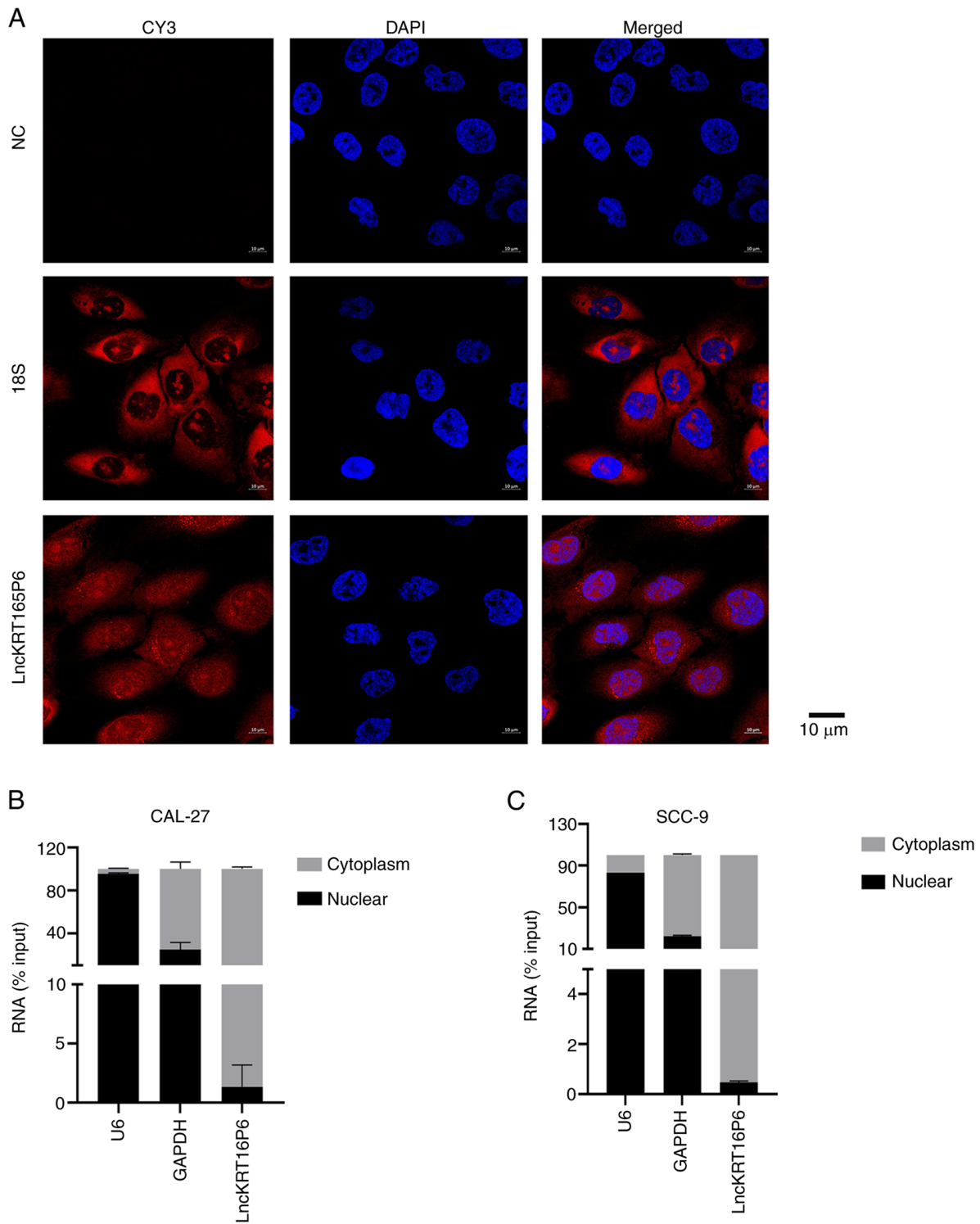


Figure 7. Intracellular distribution of lncKRT16P6. (A) Fluorescence *in situ* hybridization analysis of lncKRT16P6 localization. Scale bar=10 μ m. (B) Analysis of the localization of lncKRT16P6 in CAL-27 cells by nucleocytoplasmic separation experiments and reverse transcription-quantitative PCR. (C) Analysis of the localization of lncKRT16P6 in SCC-9 cells by nucleocytoplasmic separation experiments and reverse transcription-quantitative PCR. All data are presented as the mean \pm standard error of the mean of three independent experiments. lnc, long noncoding RNA; NC, negative control.

Co., Ltd.), N-cadherin (1:1,000; cat. no. 13116; CST Biological Reagents Co., Ltd.), Vimentin (1:1,000; #5741; CST Biological Reagents Co., Ltd.), GATAD2A (1:2,000; cat. no. ab188472, Abcam), Cyclin A (1:1,000; cat. no. WL01841, Wanleibio Co., Ltd.), Cyclin D1 (1:1,000; cat. no. WL01435a, Wanleibio Co., Ltd.), Cyclin E (1:500; cat. no. WL01072, Wanleibio Co., Ltd.), Cyclin-dependent kinase 2 (CDK2; 1:1,000; cat. no. WL01543,

Wanleibio Co., Ltd.), GAPDH (1:10,000; cat. no. 60004-1-Ig, ProteinTech Group, Inc.), β -Actin (1:1,000; cat. no. 3700; CST Biological Reagents Co., Ltd.) and β -Tubulin (1:10,000; cat. no. BS1482M, Bioworld Technology). Since each target protein had a different molecular weight distribution, in order not to overlap with the experimental protein in each case, three different loading controls were used (GAPDH, β -tubulin, β -actin) in this

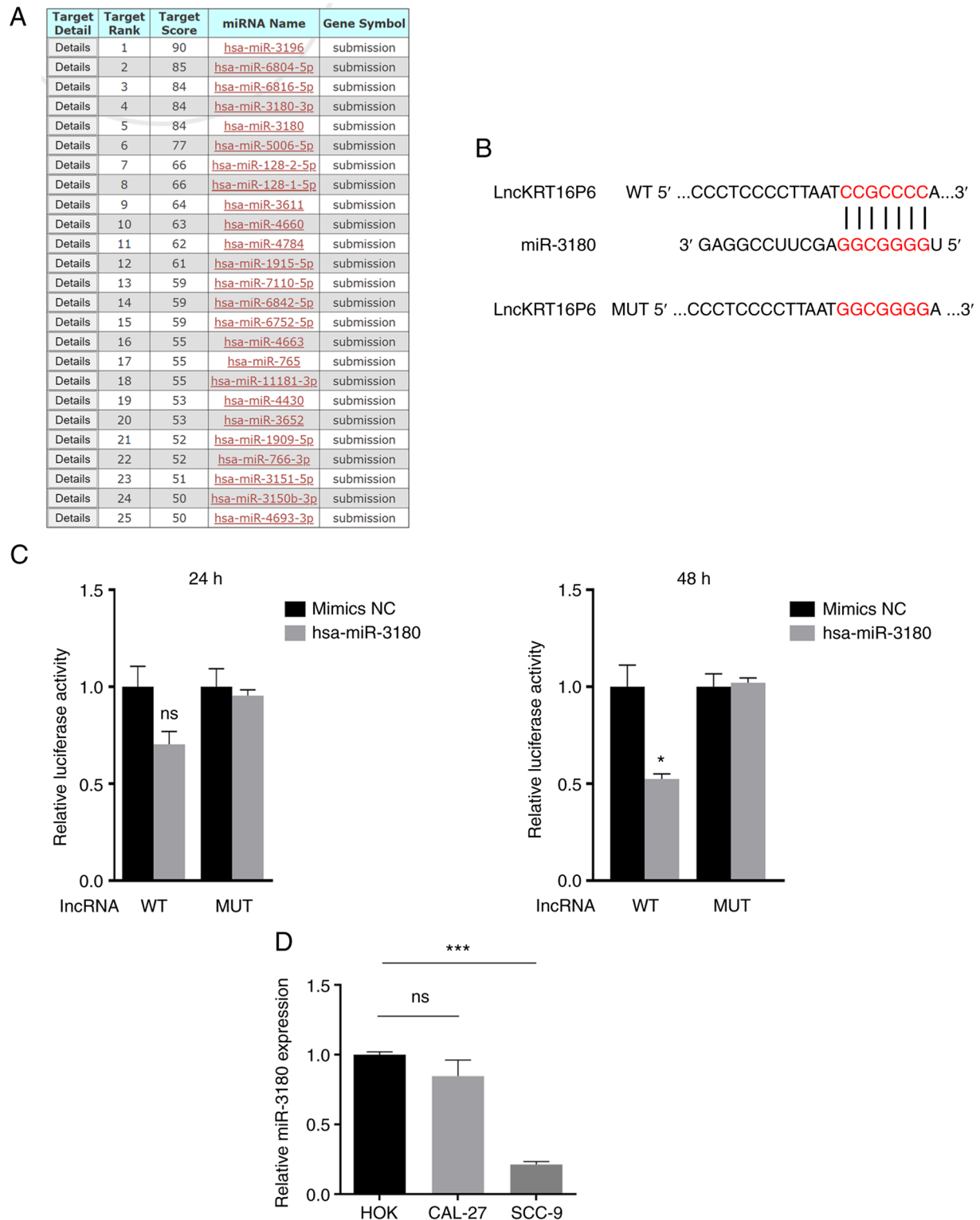


Figure 8. lncKRT16P6 acts as a ceRNA and absorbs hsa-miR-3180. (A) The miRDB database was used to predict miRNAs that may bind lncKRT16P6. (B) The binding sites between lncKRT16P6 and miR-3180 were predicted by the miRDB database. (C) A dual-luciferase reporter assay was used to detect luciferase activities in 293(T) cells cotransfected with luciferase reporter constructs containing WT or MUT lncKRT16P6 and the miR-3180 mimic. (D) The expression of miR-3180 was detected via reverse transcription-quantitative PCR in CAL-27 cells, SCC-9 cells and HOK cells. All data are presented as the mean \pm standard error of the mean of three independent experiments. * $P < 0.05$, *** $P < 0.001$. lnc, long noncoding RNA; ceRNA, competitive endogenous RNA; miR, microRNA; MUT, mutant; WT, wild type; NC, negative control.

experiment. Horseradish peroxidase-conjugated secondary antibodies, including goat anti-mouse (1:5,000; cat. no. SA00001-1) and goat anti-rabbit (1:5,000; cat. no. SA00001-2) antibodies were purchased from ProteinTech Group, Inc. Immunoreactions

were visualized by electrochemiluminescence using a BeyoECL Moon kit (Beyotime Institute of Biotechnology). Then western blot analysis was performed with the ImageJ software (v1.44p; National Institutes of Health).

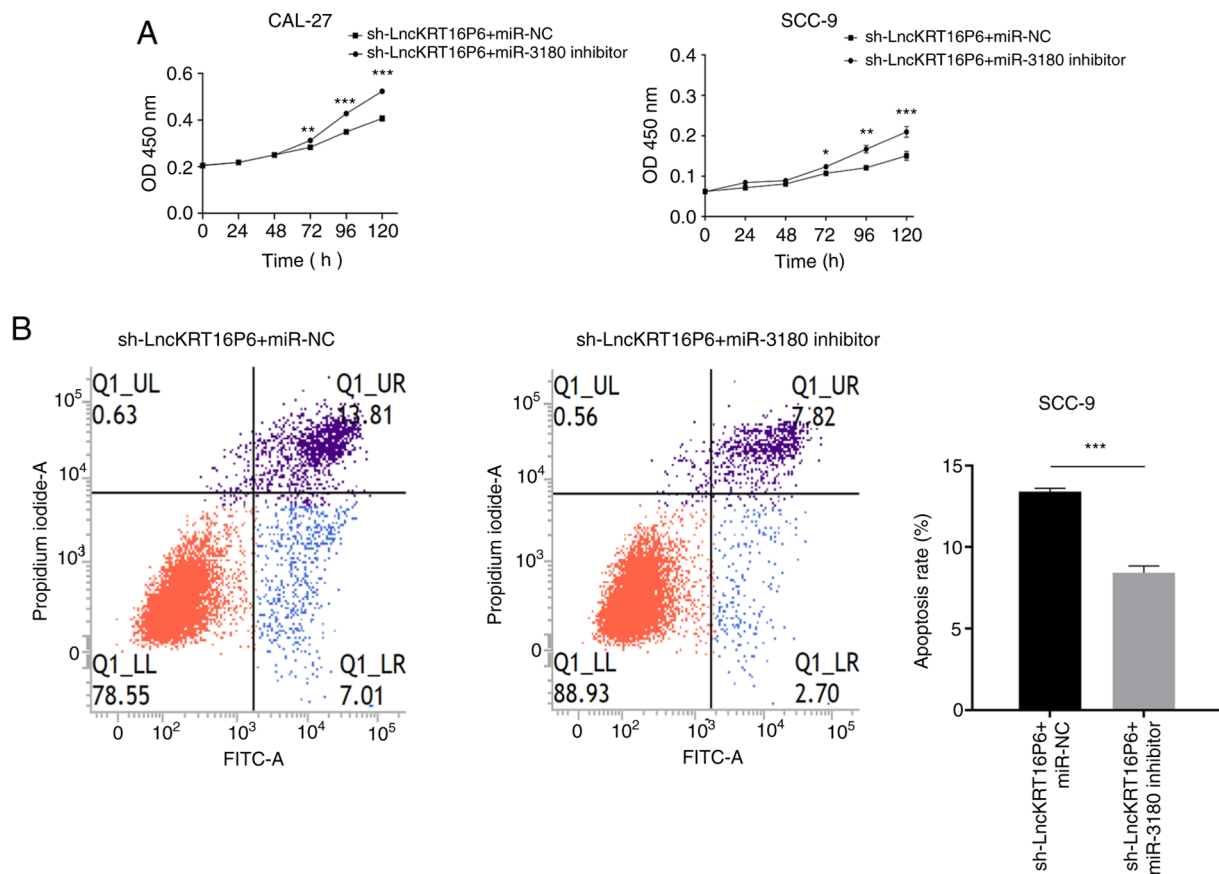


Figure 9. Depletion of hsa-miR-3180 reverses sh-LncKRT16P6-induced attenuation of TSCC cell proliferation and inhibits apoptosis. (A) CCK-8 assays were performed in CAL-27 and SCC-9 cells stably transfected with sh-LncKRT16P6 with or without the miR-3180 inhibitor. (B) Apoptosis assays were performed in SCC-9 cells stably transfected with sh-LncKRT16P6 with or without the miR-3180 inhibitor by flow cytometry. All data are presented as the mean \pm standard error of the mean of three independent experiments. * $P < 0.05$, ** $P < 0.01$, *** $P < 0.001$. miR, microRNA; sh, short hairpin; lnc, long noncoding RNA; NC, negative control.

Statistical analyses. Statistical analyses were performed using SPSS 22 software (IBM Corp.). For all continuous variables, Shapiro Wilk tests were used to test the normality. Experimental data are presented as the mean \pm standard error of the mean of a minimum of three biological replicates or are representative of three independent experiments with similar results. Unpaired Student's t test was used for two-group comparisons. To test for statistical significance between $>$ two groups, one-way ANOVA coupled with Dunnett T3's post-hoc test was used. The chi-square test was used to determine the statistical significance of differences in clinicopathological data. Paired Student's t test was used to determine the statistical significance of differences in the expression levels in clinical tissue samples. All statistical tests were two-sided and $P < 0.05$ was considered to indicate a statistically significant difference.

Results

Expression profile of lncKRT16P6 and correlation of lncKRT16P6 expression with clinicopathological characteristics in TSCC. Previously, we screened for differentially expressed lncRNAs by analyzing six pairs of TSCC and healthy adjacent normal tissues through high-throughput RNA sequencing (Kangchen BioTech Co., Ltd.) (24) and identified the significantly overexpressed lncRNA lncKRT16P6.

RT-qPCR was applied to detect the expression of differentially expressed lncRNAs. The expression level of lncKRT16P6 was determined in 50 paired human TSCC and normal tissues and lncKRT16P6 expression was consistently upregulated in the cancerous samples compared with their corresponding normal tissues ($P < 0.001$; Fig. 1A). Notably, high lncKRT16P6 expression was significantly correlated with stage I-II disease ($P = 0.0209$) and advanced tumor grade ($P = 0.0414$; Table I). Consistent with the above results, the expression of lncKRT16P6 was dramatically increased in the human tongue cancer cell lines CAL-27 and SCC-9 compared with the normal human oral keratinocyte cell line HOK (Fig. 1B). In addition, Ensembl database analysis indicated that lncKRT16P6 is located on chromosome 17 with a total length of 715 bp and its sequence was predicted to exhibit lower protein-coding potential (coding probability, 0.04 by Coding Potential Calculator 2; <http://cpc2.gao-lab.org/>) compared with those of the classical lncRNA H19, XIST and coding genes (TP53 and MYC; Fig. 1).

Depleting lncKRT16P6 inhibits TSCC progression in vitro and in vivo. To explore the role of lncKRT16P6 in TSCC cells, two specific siRNA oligonucleotides to target lncKRT16P6 in CAL-27 and SCC-9 cells were designed (Fig. 2A-B). The CCK-8 assay showed that knockdown of lncKRT16P6 significantly reduced the proliferation ability of CAL-27 and SCC-9

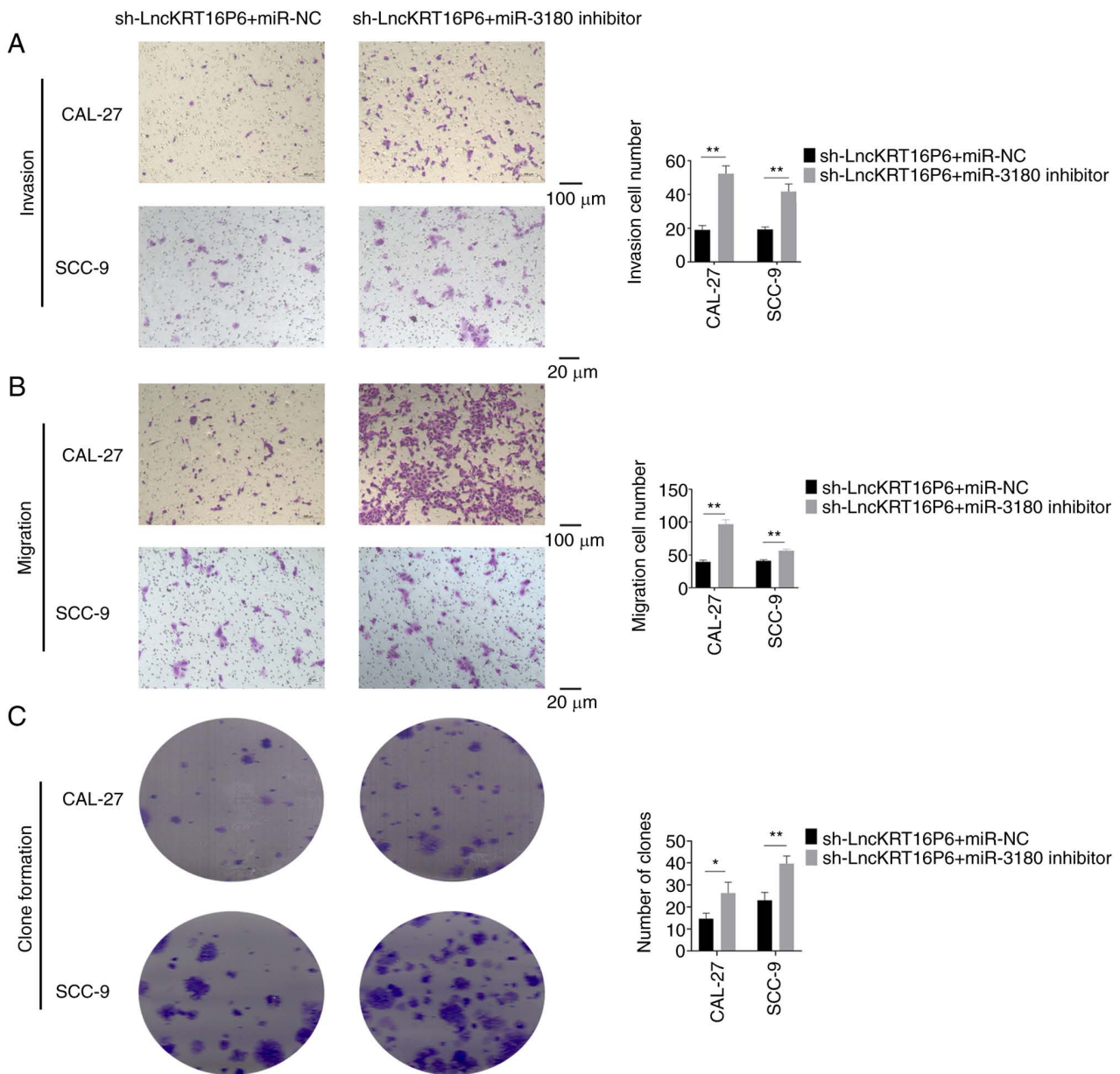


Figure 10. Depletion of hsa-miR-3180 reverses sh-lncKRT16P6-induced attenuation of TSCC cell invasion, migration and proliferation. (A) Transwell invasion assays were performed in CAL-27 and SCC-9 cells stably transfected with sh-lncKRT16P6 with or without the miR-3180 inhibitor. Scale bar=100 μ m (CAL-27 groups) or 20 μ m (SCC-9 groups). (B) Transwell migration assays were performed in CAL-27 and SCC-9 cells stably transfected with sh-lncKRT16P6 with or without the miR-3180 inhibitor. Scale bar=100 μ m (CAL-27 groups) or 20 μ m (SCC-9 groups). (C) Colony formation assays were performed in CAL-27 and SCC-9 cells stably transfected with sh-lncKRT16P6 with or without the miR-3180 inhibitor. Magnification, $\times 10$. All data are presented as the mean \pm standard error of the mean of three independent experiments. * $P < 0.05$, ** $P < 0.01$. miR, microRNA; sh, short hairpin; lnc, long noncoding RNA; NC, negative control.

cells (Fig. 2C-D) and the Transwell and colony formation assay results showed that knockdown of lncKRT16P6 significantly reduced the invasion, migration and colony-forming abilities of CAL-27 and SCC-9 cells (Fig. 3). Moreover, the flow cytometry results indicated that knockdown of lncKRT16P6 induced apoptosis (Fig. 4) and affected cell cycle progression in CAL-27 and SCC-9 cells; most of the cells arrested in G_0/G_1 phase (Fig. 5).

To further investigate the role of lncKRT16P6, CAL-27 cells with stable knockdown of lncKRT16P6 were generated (Supplementary Fig. 1B-C). Moreover, to further determine the potential role of lncKRT16P6 in the progression of TSCC, an *in vivo* model of subcutaneous tumorigenesis was established in nude mice. CAL-27 cells

with stable lncKRT16P6 knockdown or CAL-27 cells transfected with the control vector were inoculated into the right flanks of nude mice ($n=4$ mice per group). Markedly, 24 days after injection, lncKRT16P6 knockdown was found to suppress the tumorigenic and proliferation abilities of tongue cancer cells (Fig. 6A). The volumes of the subcutaneous tumors were significantly smaller in the lncKRT16P6 knockdown group compared with the control group (Fig. 6B). HE and IHC staining indicated that the model of subcutaneous tumorigenesis had been successfully established in nude mice and that the tumor tissue was Ki-67-positive (Fig. 6). Collectively, the findings suggested that lncKRT16P6 may promote the progression of tongue cancer.

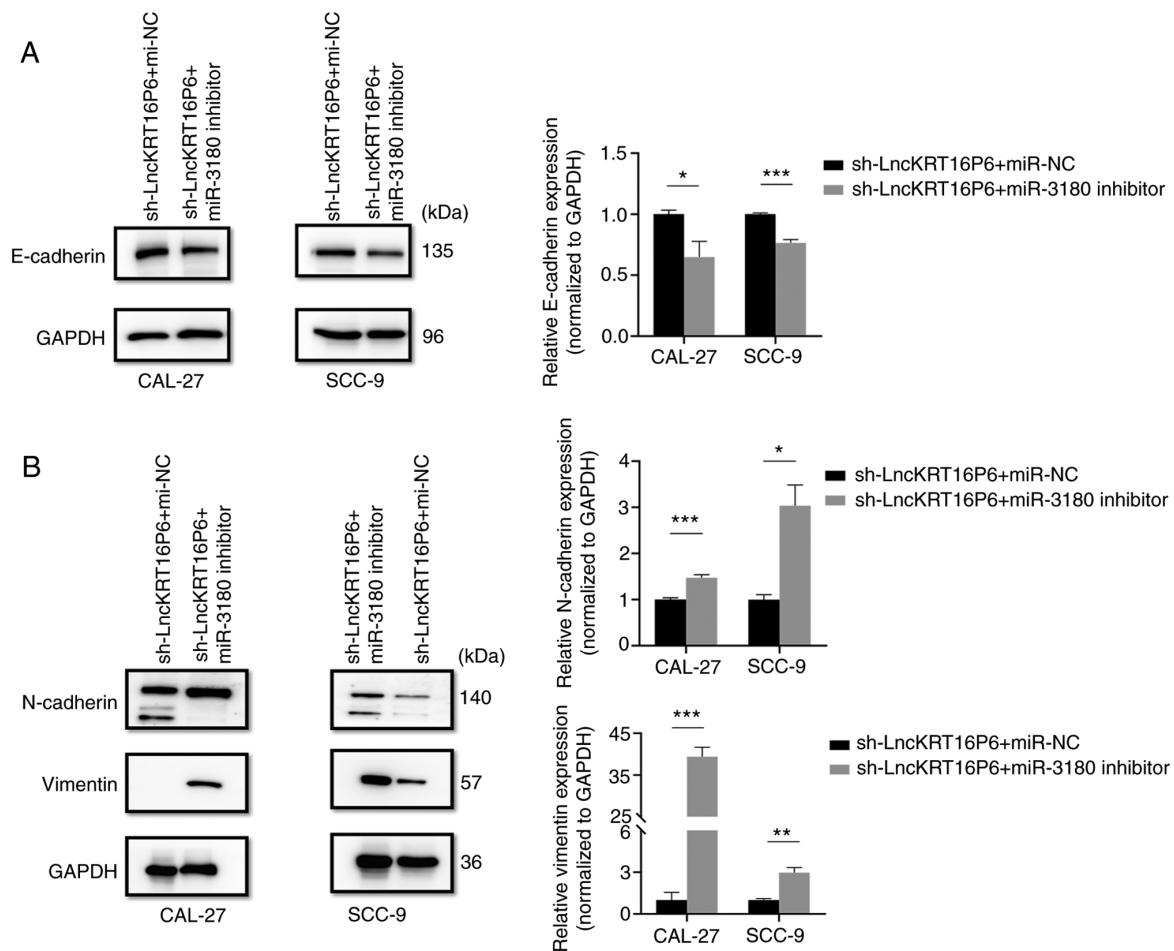


Figure 11. Depletion of hsa-miR-3180 reverses sh-LncKRT16P6-induced expression of invasion and migration-related proteins in TSCC cells. (A) Expression of the E-cadherin protein in CAL-27 and SCC-9 cells stably transfected with sh-LncKRT16P6 with or without the miR-3180 inhibitor was detected by western blotting analysis. (B) Expression of the N-cadherin and Vimentin proteins in CAL-27 and SCC-9 cells stably transfected with sh-LncKRT16P6 with or without the miR-3180 inhibitor was detected by western blotting analysis. All data are presented as the mean \pm standard error of the mean of three independent experiments. * $P < 0.05$, ** $P < 0.01$, *** $P < 0.001$. miR, microRNA; sh, short hairpin; lnc, long noncoding RNA; NC, negative control.

lncKRT16P6 functions as a ceRNA to sponge hsa-miR-3180. Next, the molecular mechanism of *lncKRT16P6* in TSCC was investigated and FISH and cell nucleocytoplasmic fractionation used to determine its localization. *lncKRT16P6* was localized mainly in the cytoplasm (Fig. 7), suggesting that it may function by acting as a sponge for various miRNAs. MiRDB was used to predict potential target miRNAs (Fig. 8A) and miR-3180 was selected for further investigation. To confirm the predicted interactions, dual-luciferase reporter assays were performed. Bioinformatic analysis revealed the shared miRNA response elements (MREs) between *lncKRT16P6* and hsa-miR-3180. Therefore, these MREs were mutated (MUT) and cloned into the luciferase reporter gene in place of the wild-type (WT) *lncKRT16P6* 3' UTR (Fig. 8B). miR-3180 directly bound *lncKRT16P6* (Fig. 8C). RT-qPCR was performed to detect miR-3180 expression in tongue cancer cell lines. The expression of miR-3180 was significantly reduced in tongue cancer cells compared with HOK cells (Fig. 8D).

Silencing hsa-miR-3180 reverses the antitumor effects of lncKRT16P6 depletion in TSCC cells. Rescue experiments were next designed to explore whether *lncKRT16P6* enhanced the malignant behavior of TSCC cells by interacting with

miR-3180. CAL-27 and SCC-9 cells were stably cotransduced with the sh-*lncKRT16P6* lentiviral vector and miR-3180 inhibitor. The inhibitory effect on miR-3180 partially attenuated the reduction in viability caused by sh-*lncKRT16P6*, as demonstrated by CCK-8 assays (Fig. 9A). Flow cytometry showed that the proportion of apoptotic cells was significantly decreased following sh-*lncKRT16P6*/miR-3180 inhibitor cotreatment (Fig. 9B). In addition, Transwell invasion and migration assays and colony formation assays demonstrated that miR-3180 partially reversed the decreases in the invasion, migration and colony formation abilities caused by *lncKRT16P6* depletion (Fig. 10). Western blot analysis was used to detect the expression of invasion- and migration-related marker proteins, such as E-cadherin, N-cadherin and Vimentin and the results were consistent with the Transwell results (Fig. 11). These findings indicate that *lncKRT16P6* promotes TSCC progression by eliminating the antitumor effects of miR-3180.

GATAD2A is a direct target of hsa-miR-3180 and acts as an oncogene in TSCC. Then, the target genes of miR-3180 in TSCC were investigated. Four databases (ENCORI, miRDB, TargetScan and miRTarBase) were used to predict potential target genes (Fig. 12A) and *GATAD2A* was selected for further

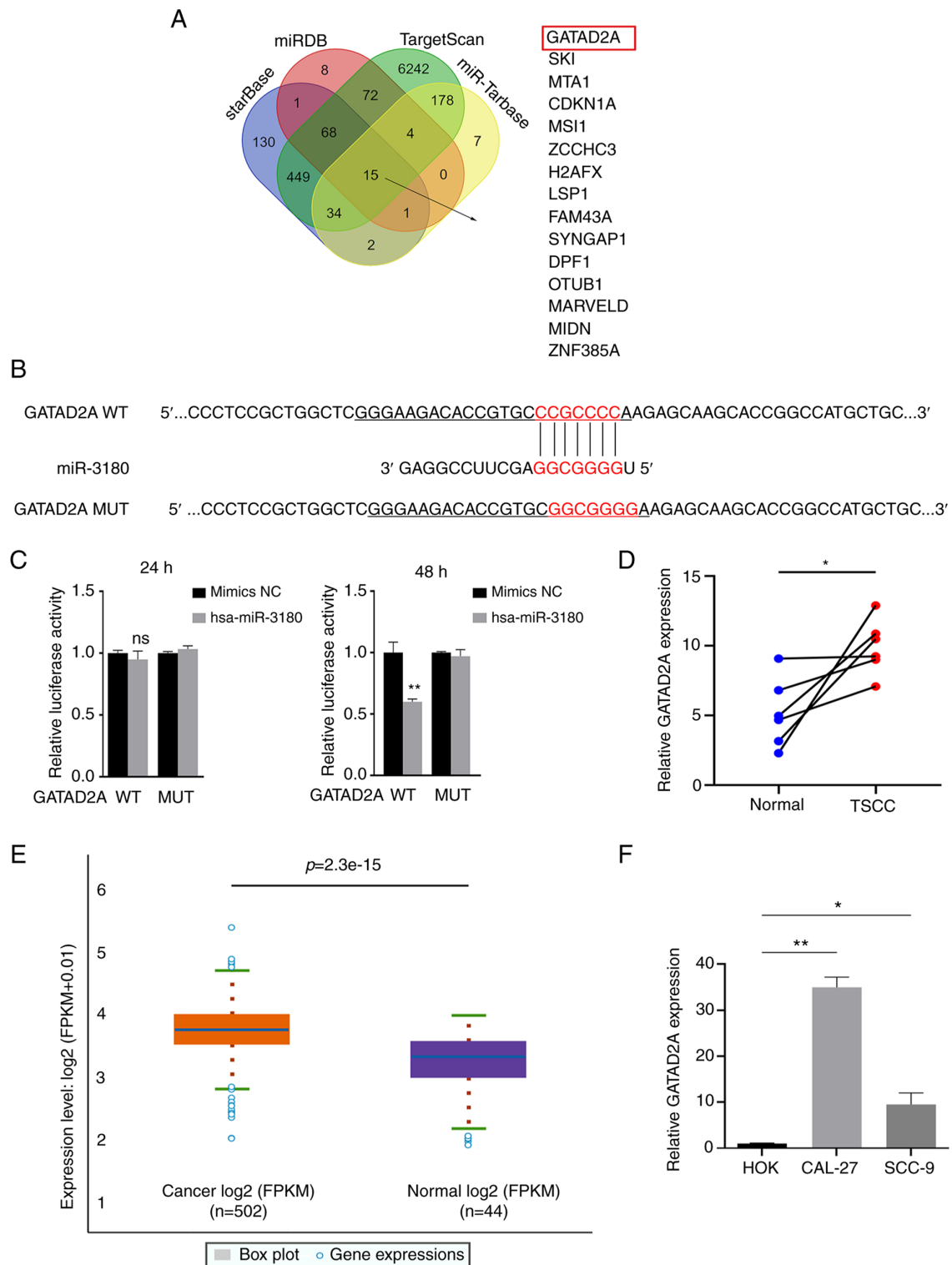


Figure 12. GATAD2A is a direct target of hsa-miR-3180. (A) Schematic showing the overlap between miR-3180 target mRNAs predicted by the ENCORI, miRDB, TargetScan and miRTarBase databases. (B) The binding sites between GATAD2A and miR-3180 were predicted by the miRDB database. (C) The dual-luciferase reporter assay detected the luciferase activities of 293(T) cells cotransfected with a luciferase reporter construct containing WT or MUT GATAD2A and the miR-3180 mimic. (D) High-throughput sequencing of GATAD2A in six pairs of TSCC and adjacent samples. (E) Expression of GATAD2A in HNSC in the ENCORI database. (F) Reverse transcription-quantitative PCR analysis was used to compare GATAD2A expression in tongue cancer and noncancerous cell lines. All data are presented as the mean \pm standard error of the mean of three independent experiments. * $P < 0.05$, ** $P < 0.01$. GATAD2A, GATA zinc finger domain containing 2A; miR, microRNA; sh, short hairpin; lnc, long noncoding RNA; WT, wild type; MUT, mutant; TSCC, tongue squamous cell carcinoma; HNSC, head and neck squamous cell carcinoma; NC, negative control.

investigation. To confirm whether GATAD2A is a potential target gene of miR-3180, 3' UTR sensors downstream of the luciferase reporter sequence were generated and cotransfected

into 293(T) cells with miR-3180 mimics. When miR-3180 was overexpressed, GATAD2A showed reduced luciferase activity (Fig. 12B and C). The expression of GATAD2A in TSCC and

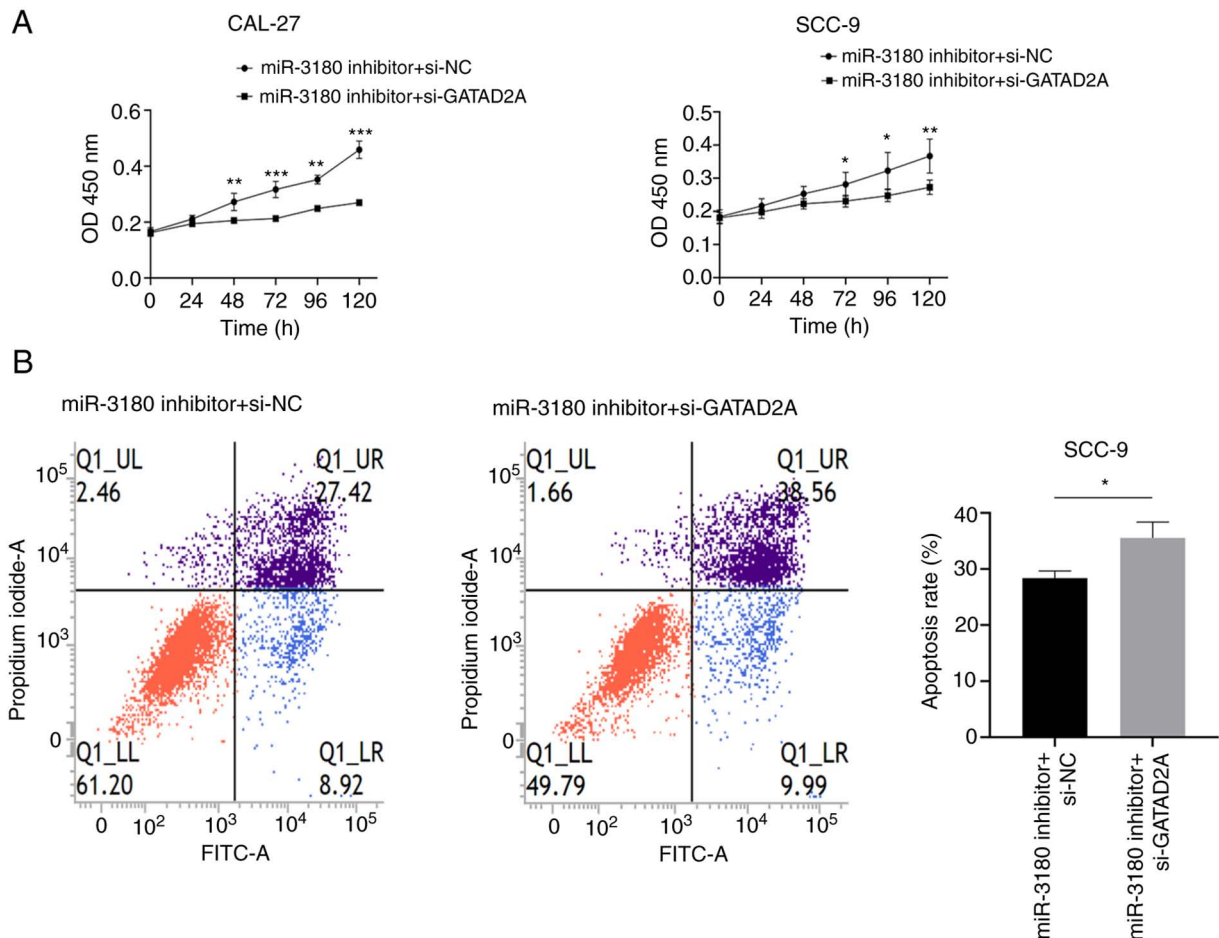


Figure 13. Depletion of GATAD2A attenuates the hsa-miR-3180 silencing-induced increase in TSCC cell proliferation and promotes apoptosis. (A) CCK-8 assays were performed in CAL-27 and SCC-9 cells transfected with the miR-3180 inhibitor with or without GATAD2A siRNAs. (B) Apoptosis assays were performed in SCC-9 cells transfected with the miR-3180 inhibitor with or without GATAD2A siRNAs by flow cytometry. All data are presented as the mean \pm standard error of the mean of three independent experiments. * $P < 0.05$, ** $P < 0.01$, *** $P < 0.001$. GATAD2A, GATA zinc finger domain containing 2A; miR, microRNA; TSCC, tongue squamous cell carcinoma; si, short interfering; NC, negative control.

head and neck squamous cell carcinoma (HNSC) tissues and cell lines was higher than that in healthy normal tissues and cells (Fig. 12D-F).

Inhibiting GATAD2A reverses the tumor-promoting effects of hsa-miR-3180 silencing in TSCC cells. Furthermore, rescue experiments were performed to verify whether miR-3180 serves a role in TSCC by interacting with GATAD2A. CAL-27 and SCC-9 cells were stably cotransfected with the miR-3180 inhibitor and GATAD2A siRNAs. The transfection efficiency of miR-3180 inhibitor, miR-3180 mimics and GATAD2A siRNAs were verified in CAL-27 and SCC-9 cells (Fig. S2). One (si-2) of the two siRNAs against GATAD2A was used in the subsequent experiments after verifying the transfection efficiency. The inhibitory effect on GATAD2A may reverse the increase in cell viability induced by the miR-3180 inhibitor, as demonstrated by CCK-8 assays (Fig. 13A). Flow cytometric analysis showed that the proportion of apoptotic cells was significantly increased following si-GATAD2A/miR-3180 inhibitor cotreatment (Fig. 13B). In addition, Transwell invasion and migration assays and colony formation assays demonstrated that GATAD2A partially attenuated the increases in promotion of migration and invasion caused by

miR-3180 depletion (Fig. 14). These findings indicated that miR-3180 inhibits TSCC progression by interacting with GATAD2A.

lncKRT16P6 acts as a decoy of hsa-miR-3180 to upregulate GATAD2A. Further experiments were performed to confirm the regulatory relationship among lncKRT16P6, GATAD2A and miR-3180 and found that the miR-3180 mimic down-regulated lncKRT16P6 expression, but knockdown of miR-3180 rescued lncKRT16P6 expression (Fig. 15A). In parallel, lncKRT16P6 expression was decreased after GATAD2A knockdown and was increased when miR-3180 was inhibited (Fig. 15B). Moreover, it was verified that the miR-3180 mimic downregulated GATAD2A expression, but the knockdown of miR-3180 rescued GATAD2A expression (Fig. 15C and D). GATAD2A expression was decreased after lncKRT16P6 knockdown and was increased when miR-3180 was inhibited (Fig. 15E and F). Moreover, in experiments to confirm the effect of lncKRT16P6 on the cell cycle in TSCC, it was found that the expression of CDK2, Cyclin A, Cyclin D1 and Cyclin E decreased following lncKRT16P6 knockdown (Fig. 16). Taken together, these data revealed that lncKRT16P6 serves as a ceRNA and sponges miR-3180,

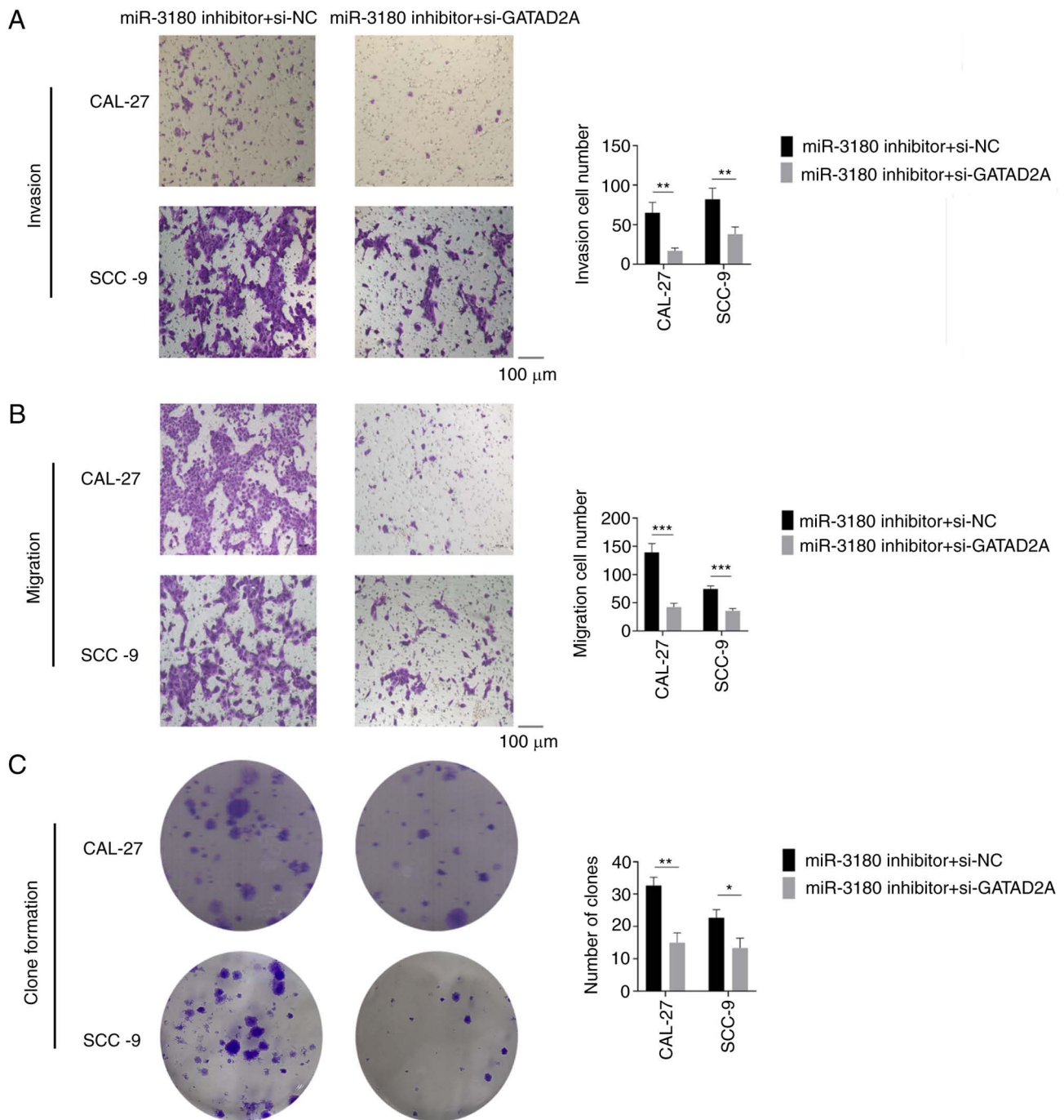


Figure 14. Depletion of GATAD2A attenuates the hsa-miR-3180 silencing-induced increase in TSCC cell invasion, migration and proliferation. Transwell (A) invasion and (B) migration assays were performed in CAL-27 and SCC-9 cells transfected with the miR-3180 inhibitor with or without GATAD2A siRNAs. Scale bar=100 μ m. (C) Colony formation assays were performed in CAL-27 and SCC-9 cells transfected with the miR-3180 inhibitor with or without GATAD2A siRNAs. Magnification, $\times 10$. All data are presented as the mean \pm standard error of the mean of three independent experiments. * $P < 0.05$, ** $P < 0.01$, *** $P < 0.001$. GATAD2A, GATA zinc finger domain containing 2A; miR, microRNA; TSCC, tongue squamous cell carcinoma; si, short interfering; NC, negative control.

leading to enhanced GATAD2A expression to regulate tongue cancer progression.

Discussion

Recently, noncoding RNAs have been gradually used to elucidate the mechanisms of tumorigenesis and tumor progression. lncRNAs are a type of noncoding RNA that mediate gene expression and they are closely associated

with a variety of tumors, including lung, gastric, colorectal and bladder tumors (27-31). The differential expression of lncRNAs is significantly associated with tumor proliferation, differentiation and metastasis, TNM stage and other clinical characteristics (32). Therefore, lncRNAs may provide new insights for exploring tumor pathogenesis and serve as potential biomarkers for multiple types of cancers. While lncRNAs have been widely studied in the development of TSCC, the pathogenic mechanism is not completely clear.

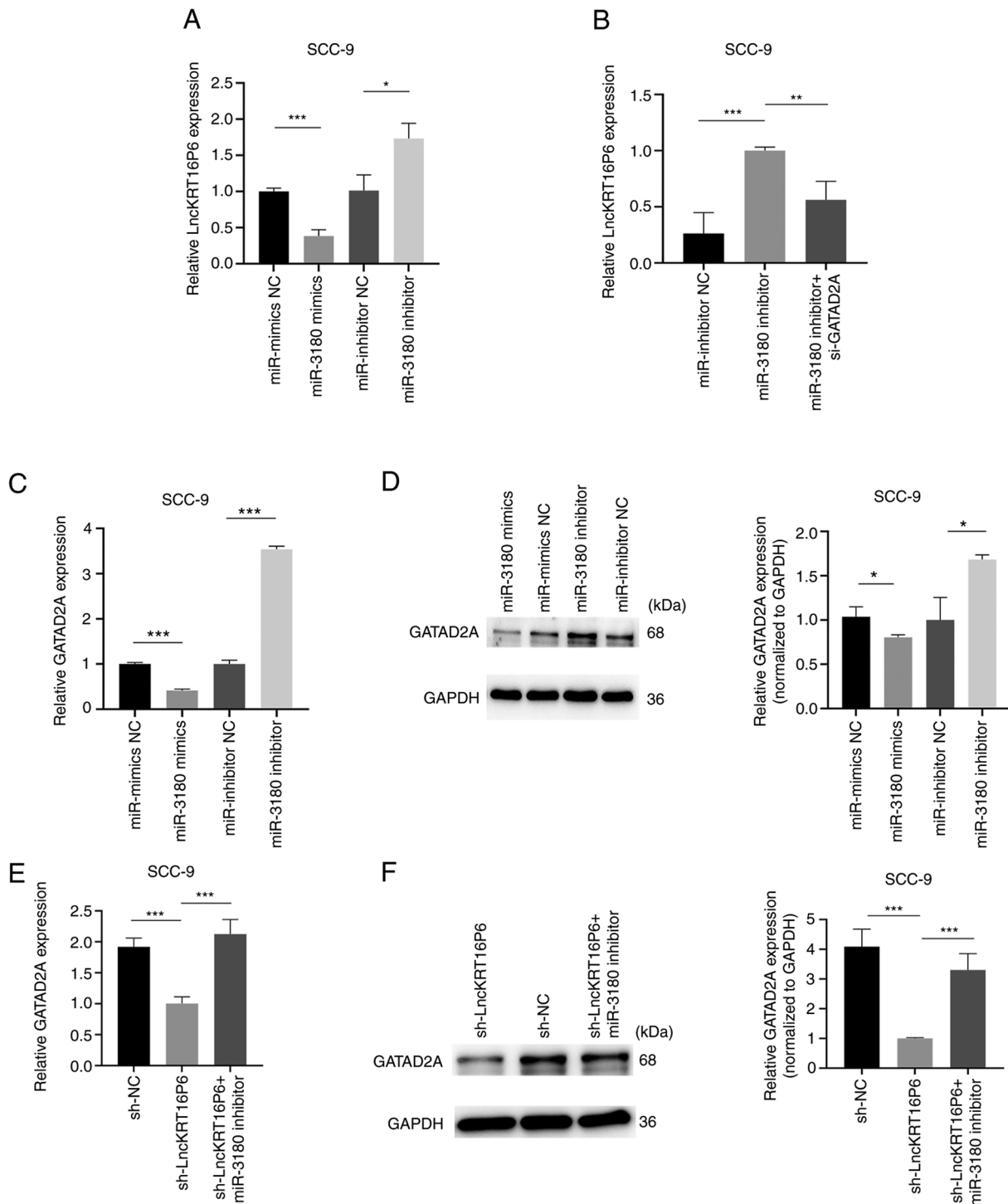


Figure 15. InKnRT16P6 acts as a decoy of hsa-miR-3180 to upregulate GATAD2A. (A) Cells were transfected with the miR-3180 mimic or inhibitor and the InKnRT16P6 level was then measured by RT-qPCR analysis. (B) Cells were cotransfected with the miR-3180 inhibitor and GATAD2A siRNAs and the InKnRT16P6 level was then measured by RT-qPCR analysis. Cells were transfected with the miR-3180 mimic or inhibitor and the GATAD2A level was then measured by (C) RT-qPCR and (D) western blotting analysis. Cells were cotransfected with sh-InKnRT16P6 and the miR-3180 inhibitor and the GATAD2A level was then measured by (E) RT-qPCR and (F) western blotting analysis. All data are presented as the mean \pm standard error of the mean of three independent experiments. * $P < 0.05$, ** $P < 0.01$, *** $P < 0.001$. InKn, long noncoding RNA; miR, microRNA; GATAD2A, GATA zinc finger domain containing 2A; RT-qPCR, reverse transcription-quantitative PCR; si, short interfering; NC, negative control.

The present study screened dysregulated lncRNAs associated with TSCC and identified a novel lncRNA, InKnRT16P6. The evidence suggested that InKnRT16P6 is an oncogenic lncRNA and is closely associated with tumor stage and differentiation grade. The present study used two cell lines commonly employed in most research and other tongue cancer

cell lines will be used in follow-up research to further verify the results of the present study and ultimately improve the experimental conclusions. The oncogenic role of InKnRT16P6 revealed *in vitro* and *in vivo* in the present study highlights the potential implication of this lncRNA as a predictive biomarker and therapeutic target for TSCC.

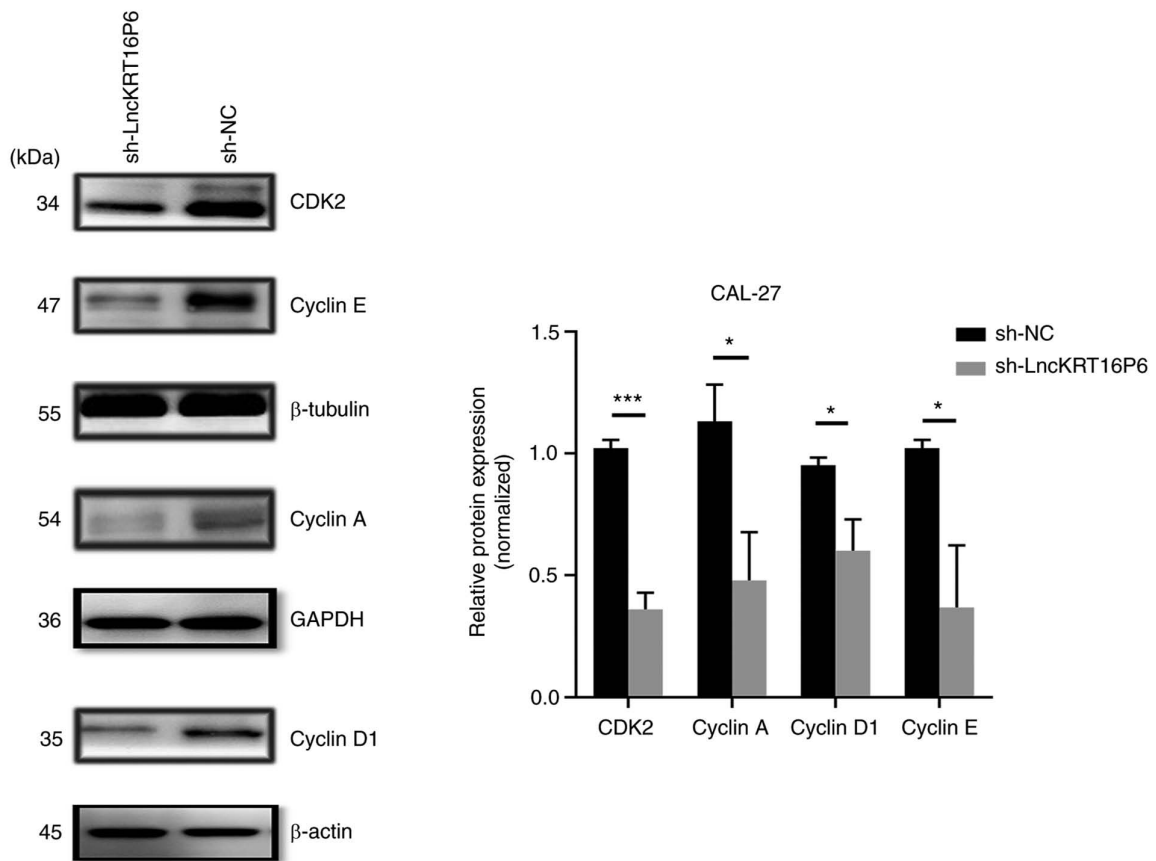


Figure 16. lncKRT16P6 promotes cyclin protein expression. Cells were transfected with sh-NC or sh-lncKRT16P6 and CDK2, Cyclin A, Cyclin D1 and Cyclin E levels were measured by western blotting analysis. All data are presented as the mean ± standard error of the mean of three independent experiments. *P<0.05, ***P<0.001. lnc, long noncoding RNA; sh, short hairpin; NC, negative control.

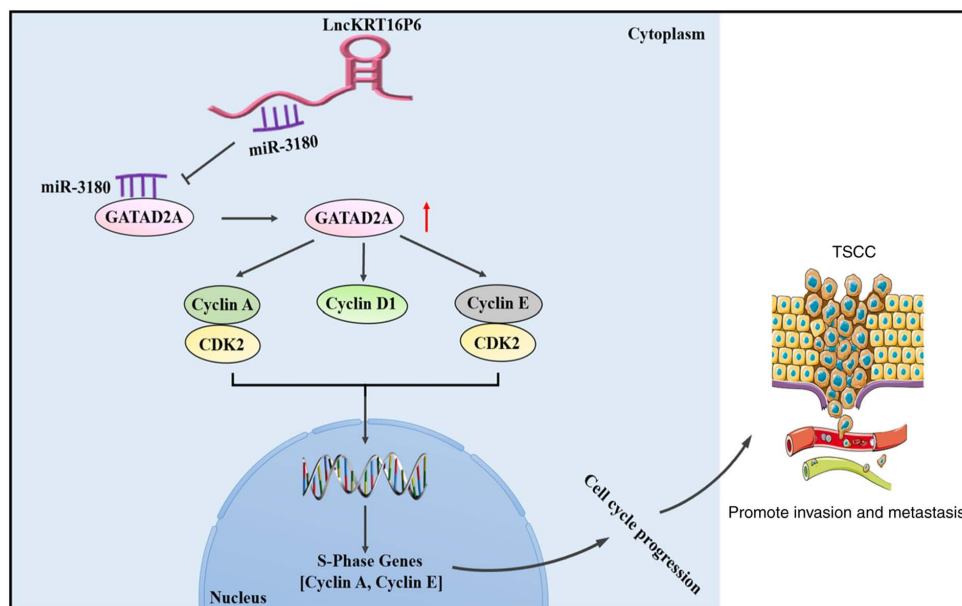


Figure 17. Graphical illustration of the mechanism by which lncKRT16P6 modulates tumor proliferation, invasion and migration in TSSC. lnc, long noncoding RNA; miR, microRNA; GATAD2A, GATA zinc finger domain containing 2A; TSSC, tongue squamous cell carcinoma.

CeRNAs mediate gene expression and are assumed to function through MREs to form a transcriptional regulatory network in which mRNAs, pseudogenes and lncRNAs may ‘interact’ with each other, which may affect the progression

of certain diseases (33,34). Studies have shown that ceRNAs serve pivotal roles in the invasion, proliferation and metastasis of cancer cells (35,36) and have confirmed that lncRNAs are also involved in regulating tumor ceRNA networks (37-40).

The present study found that lncKRT16P6 was located mainly in the cytoplasm of TSCC cells and acted as a sponge for miR-3180. In addition, the findings revealed the significance of the interaction between lncKRT16P6 and miR-3180 in tumorigenesis. The present study found that miR-3180 partially reversed the oncogenic role of lncKRT16P6.

In general, as ceRNAs, the functions of lncRNAs depend on the miRNA target (41-43). Using an online database, GATAD2A was predicted a potential target of miR-3180, which was confirmed by a luciferase reporter assay. Furthermore, overexpression of miR-3180 inhibited GATAD2A mRNA and protein expression. GATAD2A is located on chromosome 19 in humans and is a key member of the MBD2-NuRD complex (44). GATAD2A interacts with MBD2 to recruit the deacetylase core of the NuRD complex to repress target genes (45,46). Several studies have verified that GATAD2A promotes the progression of thyroid, breast and papillary thyroid cancers (47-49) and confirmed that the NuRD complex is closely associated with the G₁/S cell cycle checkpoint (50). The present study demonstrated that lncKRT16P6 upregulated GATAD2A expression by competitively sponging miR-3180, thus affecting the proliferation and metastasis of TSCC cells. Furthermore, it indicated that lncKRT16P6 can activate the expression of CDK2, Cyclin A, Cyclin D1 and Cyclin E, thus promoting the activity of the G₁/S checkpoint signaling pathways, which promote malignant behavior.

In conclusion, the present study identified lncKRT16P6 as an oncogenic lncRNA involved in TSCC development and progression. Functional and mechanistic analyses revealed that lncKRT16P6 promoted the malignant behavior of TSCC cells by acting as a ceRNA that sponges miR-3180, leading to enhanced GATAD2A expression. Moreover, depletion of lncKRT16P6 inactivated G₁/S checkpoint signaling (Fig. 17). The present study demonstrated that lncKRT16P6 serves an essential role in TSCC tumorigenesis and progression and highlighted its importance as a prognostic indicator. The identification of the lncKRT16P6/miR-3180/GATAD2A axis provides new strategies for targeted therapies for TSCC. The mechanisms by which lncKRT16P6 simultaneously affects the expression of cyclins to regulate tumor progression warrant further investigation. Furthermore, RNAscope experiments could allow highly specific quantitative analysis of nucleic acid in situ hybridization at the single-cell and single-molecule levels; this experiment will be conducted in follow-up research to continuously improve on the present results.

The present study also had certain limitations. First, the reason for the increase in lncKRT16P6 has not been clarified in the current study. Furthermore, the molecular mechanism by which GATAD2A and cyclin interact has not been clarified. These unanswered questions will be the focus of future research and will be addressed by complementary experiments in the future.

Acknowledgments

The authors thank the Public Technology Service Center of Fujian Medical University for their support.

Funding

The present study was supported by the National Natural Science Foundation of China (grant no. 81771126) and the

Science and Technology Planning Project of Fujian Province (grant no. 2019Y9031).

Availability of data and materials

All data generated or analyzed during this study are included in this published article.

Authors' contributions

MZ and LW confirm the authenticity of all the raw data. Research design and implementation: MZ and LW designed and implemented the study and performed data analysis and interpretation. MZ, LW and XW performed statistical analysis. MZ wrote the manuscript, JC revised the manuscript and supervised the study and helped to solve various problems in the research. All authors read and approved the final manuscript.

Ethics approval and consent to participate

The study protocol was approved by the Ethics Committee of the First Affiliated Hospital of Fujian Medical University [approval number: 159 (2020) of the First Affiliated Hospital of Fujian Medical University]. Written informed consent was obtained from all participants in accordance with the Declaration of Helsinki.

Patient consent for publication

Not applicable.

Competing interests

The authors declare that they have no competing interests.

References

- Mannelli G, Arcuri F, Agostini T, Innocenti M, Raffaini M and Spinelli G: Classification of tongue cancer resection and treatment algorithm. *J Surg Oncol* 117: 1092-1099, 2018.
- Sagheb K, Kumar V, Rahimi-Nedjat R, Dollhausen M, Ziebart T, Al-Nawas B and Walter C: Cervical metastases behavior of T1-2 squamous cell carcinoma of the tongue. *J Maxillofac Oral Surg* 16: 300-305, 2017.
- Chen X, Xie R, Gu P, Huang M, Han J, Dong W, Xie W, Wang B, He W, Zhong G, *et al*: Long noncoding RNA LBCS inhibits self-renewal and chemoresistance of bladder cancer stem cells through epigenetic silencing of SOX2. *Clin Cancer Res* 25: 1389-1403, 2019.
- Yue B, Cai D, Liu C, Fang C and Yan D: Linc00152 functions as a competing endogenous RNA to confer oxaliplatin resistance and holds prognostic values in colon cancer. *Mol Ther* 24: 2064-2077, 2016.
- Djebali S, Davis CA, Merkel A, Dobin A, Lassmann T, Mortazavi A, Tanzer A, Lagarde J, Lin W, Schlesinger F, *et al*: Landscape of transcription in human cells. *Nature* 489: 101-108, 2012.
- Wang KC and Chang HY: Molecular mechanisms of long noncoding RNAs. *Mol Cell* 43: 904-914, 2011.
- Chu C, Spitale RC and Chang HY: Technologies to probe functions and mechanisms of long noncoding RNAs. *Nat Struct Mol Biol* 22: 29-35, 2015.
- Batista PJ and Chang HY: Long noncoding RNAs: Cellular address codes in development and disease. *Cell* 152: 1298-1307, 2013.
- Zhang G, Li S, Lu J, Ge Y, Wang Q, Ma G, Zhao Q, Wu D, Gong W, Du M, *et al*: LncRNA MT1JP functions as a ceRNA in regulating FBXW7 through competitively binding to miR-92a-3p in gastric cancer. *Mol Cancer* 17: 87, 2018.

10. Yi W, Li J, Zhu X, Wang X, Fan L, Sun W, Liao L, Zhang J, Li X, Ye J, *et al.*: CRISPR-assisted detection of RNA-protein interactions in living cells. *Nat Methods* 17: 685-688, 2020.
11. Long Y, Wang X, Youmans DT and Cech TR: How do lncRNAs regulate transcription? *Sci Adv* 3: eaao2110, 2017.
12. Wang J, Zhang X, Chen W, Hu X, Li J and Liu C: Regulatory roles of long noncoding RNAs implicated in cancer hallmarks. *Int J Cancer* 146: 906-916, 2019.
13. Gupta RA, Shah N, Wang KC, Kim J, Horlings HM, Wong DJ, Tsai MC, Hung T, Argani P, Rinn JL, *et al.*: Long non-coding RNA HOTAIR reprograms chromatin state to promote cancer metastasis. *Nature* 464: 1071-1076, 2010.
14. Zhang S, Ma H, Zhang D, Xie S, Wang W, Li Q, Lin Z and Wang Y: LncRNA KCNQ1OT1 regulates proliferation and cisplatin resistance in tongue cancer via miR-211-5p mediated Ezrin/Fak/Src signaling. *Cell Death Dis* 9: 742, 2018.
15. Su SC, Yeh CM, Lin CW, Hsieh YH, Chuang CY, Tang CH, Lee YC and Yang SF: A novel melatonin-regulated lncRNA suppresses TPA-induced oral cancer cell motility through replenishing PRUNE2 expression. *J Pineal Res* 71: e12760, 2021.
16. Zhang F, Wang H, Yu J, Yao X, Yang S, Li W, Xu L and Zhao L: LncRNA CRNDE attenuates chemoresistance in gastric cancer via SRSF6-regulated alternative splicing of PICALM. *Mol Cancer* 20: 6, 2021.
17. Kristensen LS, Andersen MS, Stagsted LV, Ebbesen KK, Hansen TB and Kjems J: The biogenesis, biology and characterization of circular RNAs. *Nat Rev Genet* 20: 675-691, 2019.
18. Liu J, Mayekar MK, Wu W, Yan M, Guan H, Wang J, Zaman A, Cui Y, Bivona TG, Choudhry H, *et al.*: Long non-coding RNA ESCAL-1 promotes esophageal squamous cell carcinoma by down regulating the negative regulator of APOBEC3G. *Cancer Lett* 493: 217-227, 2020.
19. Zheng ZQ, Li ZX, Zhou GQ, Lin L, Zhang LL, Lv JW, Huang XD, Liu RQ, Chen F, He XJ, *et al.*: Long noncoding RNA FAM225A promotes nasopharyngeal carcinoma tumorigenesis and metastasis by acting as ceRNA to Sponge miR-590-3p/miR-1275 and upregulate ITGB3. *Cancer Res* 79: 4612-4626, 2019.
20. Sheng X, Dai H, Du Y, Peng J, Sha R, Yang F, Zhou L, Lin Y, Xu S, Wu Y, *et al.*: LncRNA CARMN overexpression promotes prognosis and chemosensitivity of triple negative breast cancer via acting as miR143-3p host gene and inhibiting DNA replication. *J Exp Clin Cancer Res* 40: 205, 2021.
21. Jia B, Xie T, Qiu X, Sun X, Chen J, Huang Z, Zheng X, Wang Z and Zhao J: Long noncoding RNA FALEC inhibits proliferation and metastasis of tongue squamous cell carcinoma by epigenetically silencing ECM1 through EZH2. *Aging (Albany NY)* 11: 4990-5007, 2019.
22. Zhang H, Zhao L, Wang YX, Xi M, Liu SL and Luo LL: Long non-coding RNA HOTTIP is correlated with progression and prognosis in tongue squamous cell carcinoma. *Tumour Biol* 36: 8805-8809, 2015.
23. Fang Z, Zhang S, Wang Y, Shen S, Wang F, Hao Y, Li Y, Zhang B, Zhou Y and Yang H: Long non-coding RNA MALAT-1 modulates metastatic potential of tongue squamous cell carcinomas partially through the regulation of small proline rich proteins. *BMC Cancer* 16: 706, 2016.
24. Zhang M, Chen Z, Zhang S, Wu L, Jie Y, Liao Y, Huang Y, Chen J and Shi B: Analysis of differentially expressed long non-coding RNAs and the associated TF-mRNA network in tongue squamous cell carcinoma. *Front Oncol* 10: 1421, 2020.
25. Liu Y, Hu Q, Pan Y, Wang Y, Jiang L, Lin H, Lin D and Cheng H: The apoptotic and autophagic effects of cast Au-Pt, and differently manufactured Co-Cr and cp-Ti on three-dimensional oral mucosal model. *Mater Sci Eng C Mater Biol Appl* 120: 111672, 2021.
26. Livak KJ and Schmittgen TD: Analysis of relative gene expression data using real-time quantitative PCR and the 2(-Delta Delta C(T)) method. *Methods* 25: 402-408, 2001.
27. Chen Z, Chen X, Lu B, Gu Y, Chen Q, Lei T, Nie F, Gu J, Huang J, Wei C, *et al.*: Up-regulated LINC01234 promotes non-small-cell lung cancer cell metastasis by activating VAV3 and repressing BTG2 expression. *J Hematol Oncol* 13: 7, 2020.
28. Shuai Y, Ma Z, Liu W, Yu T, Yan C, Jiang H, Tian S, Xu T and Shu Y: TEAD4 modulated lncRNA MNX1-AS1 contributes to gastric cancer progression partly through suppressing BTG2 and activating BCL2. *Mol Cancer* 19: 6, 2020.
29. Xu TP, Ma P, Wang WY, Shuai Y, Wang YF, Yu T, Xia R and Shu YQ: KLF5 and MYC modulated LINC00346 contributes to gastric cancer progression through acting as a competing endogenous RNA and indicates poor outcome. *Cell Death Differ* 26: 2179-2193, 2019.
30. Chen L, He M, Zhang M, Sun Q, Zeng S, Zhao H, Yang H, Liu M, Ren S, Meng X and Xu H: The role of non-coding RNAs in colorectal cancer, with a focus on its autophagy. *Pharmacol Ther* 226: 107868, 2021.
31. Chen C, Zheng H, Luo Y, Kong Y, An M, Li Y, He W, Gao B, Zhao Y, Huang H, *et al.*: SUMOylation promotes extracellular vesicle-mediated transmission of lncRNA ELNAT1 and lymph node metastasis in bladder cancer. *J Clin Invest* 131: e146431, 2021.
32. Wu P, Mo Y, Peng M, Tang T, Zhong Y, Deng X, Xiong F, Guo C, Wu X, Li Y, *et al.*: Emerging role of tumor-related functional peptides encoded by lncRNA and circRNA. *Mol Cancer* 19: 22, 2020.
33. Tay Y, Rinn J and Pandolfi PP: The multilayered complexity of ceRNA crosstalk and competition. *Nature* 505: 344-352, 2014.
34. Salmena L, Poliseno L, Tay Y, Kats L and Pandolfi PP: A ceRNA hypothesis: The rosetta stone of a hidden RNA language? *Cell* 146: 353-358, 2011.
35. Abdollahzadeh R, Daraei A, Mansoori Y, Sepahvand M, Amoli MM and Tavakkoly-Bazzaz J: Competing endogenous RNA (ceRNA) cross talk and language in ceRNA regulatory networks: A new look at hallmarks of breast cancer. *J Cell Physiol* 234: 10080-10100, 2019.
36. Qu L, Ding J, Chen C, Wu ZJ, Liu B, Gao Y, Chen W, Liu F, Sun W, Li XF, *et al.*: Exosome-transmitted lncARSR promotes Sunitinib resistance in renal cancer by acting as a competing endogenous RNA. *Cancer Cell* 29: 653-668, 2016.
37. Li A, Mallik S, Luo H, Jia P, Lee DF and Zhao Z: H19, a long non-coding RNA, mediates transcription factors and target genes through interference of microRNAs in pan-cancer. *Mol Ther Nucleic Acids* 21: 180-191, 2020.
38. Xu J, Xiao Y, Liu B, Pan S, Liu Q, Shan Y, Li S, Qi Y, Huang Y and Jia L: Exosomal MALAT1 sponges miR-26a/26b to promote the invasion and metastasis of colorectal cancer via FUT4 enhanced fucosylation and PI3K/Akt pathway. *J Exp Clin Cancer Res* 39: 54, 2020.
39. Ji W, Diao YL, Qiu YR, Ge J, Cao XC and Yu Y: LINC00665 promotes breast cancer progression through regulation of the miR-379-5p/LIN28B axis. *Cell Death Dis* 11: 16, 2020.
40. Zhu X, Bu F, Tan T, Luo Q, Zhu J, Lin K, Huang J, Luo C and Zhu Z: Long noncoding RNA RP11-757G1.5 sponges miR-139-5p and upregulates YAP1 thereby promoting the proliferation and liver, spleen metastasis of colorectal cancer. *J Exp Clin Cancer Res* 39: 207, 2020.
41. Jia Y, Tian C, Wang H, Yu F, Lv W, Duan Y, Cheng Z, Wang X, Wang Y, Liu T, *et al.*: Long non-coding RNA NORAD/miR-224-3p/MTDH axis contributes to CDDP resistance of esophageal squamous cell carcinoma by promoting nuclear accumulation of beta-catenin. *Mol Cancer* 20: 162, 2021.
42. He Y, Jiang X, Duan L, Xiong Q, Yuan Y, Liu P, Jiang L, Shen Q, Zhao S, Yang C and Chen Y: LncRNA PKMYT1AR promotes cancer stem cell maintenance in non-small cell lung cancer via activating Wnt signaling pathway. *Mol Cancer* 20: 156, 2021.
43. Li ZY, Xie Y, Deng M, Zhu L, Wu X, Li G, Shi NX, Wen C, Huang W, Duan Y, *et al.*: c-Myc-activated intronic miR-210 and lncRNA MIR210HG synergistically promote the metastasis of gastric cancer. *Cancer Lett* 526: 322-334, 2022.
44. Sher F, Hossain M, Seruggia D, Schoonenberg VA, Yao Q, Cifani P, Dassama LM, Cole MA, Ren C, Vinjamur DS, *et al.*: Rational targeting of a NuRD subcomplex guided by comprehensive in situ mutagenesis. *Nat Genet* 51: 1149-1159, 2019.
45. Gnanaprasam MN, Scarsdale JN, Amaya ML, Webb HD, Desai MA, Walavalkar NM, Wang SZ, Zu Zhu S, Ginder GD and Williams DC Jr: p66Alpha-MBD2 coiled-coil interaction and recruitment of Mi-2 are critical for globin gene silencing by the MBD2-NuRD complex. *Proc Natl Acad Sci USA* 108: 7487-7492, 2011.
46. Desai MA, Webb HD, Sinanan LM, Scarsdale JN, Walavalkar NM, Ginder GD and Williams DC Jr: An intrinsically disordered region of methyl-CpG binding domain protein 2 (MBD2) recruits the histone deacetylase core of the NuRD complex. *Nucleic Acids Res* 43: 3100-3113, 2015.
47. Wang Z, Kang J, Deng X, Guo B, Wu B and Fan Y: Knockdown of GATAD2A suppresses cell proliferation in thyroid cancer *in vitro*. *Oncol Rep* 37: 2147-2152, 2017.
48. Lu D, Song J, Lu Y, Fall K, Chen X, Fang F, Landén M, Hultman CM, Czene K, Sullivan P, *et al.*: A shared genetic contribution to breast cancer and schizophrenia. *Nat Commun* 11: 4637, 2020.
49. Yao Y, Chen X, Yang H, Chen W, Qian Y, Yan Z, Liao T, Yao W, Wu W, Yu T, *et al.*: Hsa_circ_0058124 promotes papillary thyroid cancer tumorigenesis and invasiveness through the NOTCH3/GATAD2A axis. *J Exp Clin Cancer Res* 38: 318, 2019.
50. van den Heuvel S and Dyson NJ: Conserved functions of the pRB and E2F families. *Nat Rev Mol Cell Biol* 9: 713-724, 2008.

